The Journal of Immunology

Development and Homeostasis of T Cell Memory in Rhesus Macaque

Christine J. Pitcher, Shoko I. Hagen, Joshua M. Walker, Richard Lum, Bridget L. Mitchell, Vernon C. Maino, Michael K. Axthelm and Louis J. Picker

J Immunol 2002; 168:29-43; ;
doi: 10.4049/jimmunol.168.1.29
http://www.jimmunol.org/content/168/1/29

The Journal of Immunology is published twice each month by
The American Association of Immunologists, Inc.,
1451 Rockville Pike, Suite 650, Rockville, MD 20852

Print ISSN: 0022-1767 Online ISSN: 1550-6606.

Development and Homeostasis of T Cell Memory in Rhesus Macaque[1]

Christine J. Pitcher,[2]* Shoko I. Hagen,[2]* Joshua M. Walker,* Richard Lum,* Bridget L. Mitchell,* Vernon C. Maino,† Michael K. Axthelm,* and Louis J. Picker[3]*

The rhesus macaque (RM) is a critical animal model for studies of viral pathogenesis and immunity, yet fundamental aspects of their cellular immune response remain poorly defined. One such deficiency is the lack of validated phenotypic signatures for their naive and memory T cell subsets, and the resultant unavailability of accurate information on their memory T cell development, homeostasis, and function. In this study, we report a phenotypic paradigm allowing definitive characterization of these subsets and their comprehensive functional analysis. Naive T cells are optimally delineated by their homogeneous $CD95^{low}CD28^{high}\beta_7$ integrin^{int} ($CD4^+$) or $CD95^{low}CD28^{int}CD11a^{low}$ ($CD8^+$) phenotypes. This subset 1) was present in blood and secondary lymph tissues, but not effector sites; 2) vastly predominated in the fetal/neonatal immune system, but rapidly diminished with postnatal age; 3) lacked IFN-γ production capability, and specific responses to RM CMV; and 4) demonstrated low in vivo proliferative activity. $CD4^+$ and $CD8^+$ memory subsets were $CD95^{high}$, but otherwise phenotypically heterogeneous and included all IFN-γ production, RM CMV-specific responses, effector site T cells, and demonstrated high in vivo proliferative activity (~10 times the naive subset). These analyses also revealed the RM "effector memory" subset within the overall memory population. This population, best defined by lack of CD28 expression, contained the majority of RM CMV-specific cells, was highly enriched in extralymphoid effector sites, and comprised an increasing proportion of total memory cells with age. The effector memory subset demonstrated similar in vivo proliferative activity and survival as $CD28^+$ "central memory" T cells, consistent with independent homeostatic regulation. *The Journal of Immunology,* **2002, 168: 29–43.**

The evolution of phenotypic criteria for the delineation of human naive and memory/effector T cells over the past 12 years has revolutionized understanding of the cellular basis of immunologic memory and has greatly facilitated the investigation of T cell function and homeostasis in healthy and diseased individuals (1–7). The now well-established memory/naive paradigm holds that both $CD4^+$ and $CD8^+$ peripheral T cells can be readily divided into two major subsets: 1) an Ag inexperienced (naive) subset with a broad thymic-selected TCR repertoire, low immediate effector potential, high costimulatory requirements, low turnover, and almost exclusive recirculation through secondary lymphoid tissues; and 2) an Ag-experienced (memory/effector) subset with an Ag-selected TCR repertoire; heterogeneous, but highly differentiated, functional potential; heterogeneous, but on average low, costimulatory requirements; relatively high turnover; and the ability to broadly or selectively recirculate through the various extralymphoid tissues of the body (effector sites or potential effector sites) (4, 5, 7–10). Although in unusual circumstances memory differentiation might occur in the absence of Ag (e.g., severe lymphodepletion) (11), the vast majority of memory cells are thought to undergo the naive to memory differentiation process immediately following their first contact with and activation by Ag in secondary lymphoid tissues coincident with rapid clonal expansion (5). The functional potential of the resultant memory/effector cells is thought to be initially determined by microenvironmental conditions during the naive to memory/effector transition, but then potentially modified during subsequent encounters with Ag in diverse microenvironments (5, 12–14).

This memory/naive T cell paradigm in humans was developed by painstaking, functional analysis of phenotypically defined T cell subsets and, not surprisingly, many of the phenotypic criteria used to discriminate naive and memory subsets ultimately involve cell surface molecules whose functions reflect this paradigm. Naive T cells homogeneously express moderate to high levels of cell surface molecules involved in secondary lymphoid tissue migration (CD62L, $\alpha_4\beta_7$ integrin, CCR7) and costimulation (CD27, CD28), low levels of general adhesion molecules (CD11a, CD49d, CD58, CD2) and apoptosis-associated molecules (CD95), lack expression of molecules involved in migration to extralymphoid effector sites (cutaneous lymphocyte-associated Ag, CCR5), and express high and low levels of the RA and RO CD45 isoforms, respectively (2, 4, 15–19). In contrast, consistent with their marked functional diversity, memory cells lack a precise identifying phenotype; instead, they express complex, but stereotyped, patterns of these markers that allow clear-cut differentiation from the naive subset only with strategic multiparameter analysis (2, 4). The CD4 and CD8 lineages differ in detail, but both conform to these general principles.

The increasingly sophisticated and validated phenotypic criteria for delineating naive and memory T cell populations in humans have been effectively applied to numerous investigations of immune pathobiology, most notably in HIV disease (1, 3, 6, 20, 21). However, much less rigor has been applied to the study of T cell

*Vaccine and Gene Therapy Institute, Oregon Regional Primate Research Center, Oregon Health and Science University, West Campus, Beaverton, OR 97006; and †BD Biosciences, San Jose, CA 95131

Received for publication August 29, 2001. Accepted for publication October 24, 2001.

The costs of publication of this article were defrayed in part by the payment of page charges. This article must therefore be hereby marked *advertisement* in accordance with 18 U.S.C. Section 1734 solely to indicate this fact.

[1] This study was supported by National Institutes of Health Grants P51RR00163 and R21AI44758.

[2] C.J.P. and S.I.H. contributed equally to this work.

[3] Address correspondence and reprint requests to Dr. Louis J. Picker, Vaccine and Gene Therapy Institute, Oregon Health and Science University, West Campus, 505 NW 185th Avenue, Beaverton, OR 97006. E-mail address: pickerl@ohsu.edu

0022-1767/02/$02.00

memory in the major animal model for HIV infection, the rhesus macaque (RM).[4] Cross-reacting, human-specific reagents have been used to investigate peripheral T cell populations in these animals, but without the optimization, validation, and functional correlation that would be required for the development of accurate analytic strategies. The availability of such strategies would greatly enhance the quality of data obtained from numerous ongoing studies of SIV immuno- and pathobiology, as well as other RM infectious disease models. Moreover, this human-like animal model would appear to offer a unique, heretofore underexploited opportunity to delineate aspects of in vivo T cell physiology that, due to practical or ethical considerations, are not readily approachable in the human system. Thus, we have undertaken the task of 1) determining optimal reagents and developing validated criteria for the delineation of naive and memory T cells in RM, 2) developing analytical approaches to ascertain the function and turnover of these cells, and 3) using these criteria and tools to explore fundamental aspects of RM memory T cell development and homeostasis in vivo. We were also interested in defining those components of memory directly involved in host defense against chronic viral infection—the so-called "effector memory" subset (8, 18, 22, 23). Our results establish a strikingly rapid, coordinate development of $CD4^+$ and $CD8^+$ T cell memory in normal RMs and characterize a remarkable steady-state dynamism in the turnover of these memory populations. Moreover, these animals quickly establish and maintain high frequencies of differentiated, effector memory $CD8^+$ T cells, consistent with a requirement to maintain high levels of immune activity directed at persistent pathogens. These features are much more pronounced and time contracted than in the (western society) human, suggesting the RM model as an invaluable resource in the delineation of the fundamental mechanisms controlling T cell memory in primates.

Materials and Methods

Animals

All animals used in this study were colony-bred RM (*Macaca mulatta*) of Indian origin maintained and used in accordance with guidelines of the Animal Care and Use Committee at the Oregon Regional Primate Research Center and the *National Institutes of Health Guide for the Care and Use of Laboratory Animals*. Healthy animals of either sex were selected to represent the life span of the RM for peripheral blood analyses. Tissues were obtained from necropsied animals through the Oregon Regional Primate Research Center's Tissue Distribution Program. Unless otherwise indicated, these animals were free of known infectious or immunologic disease. Animals were anesthetized with ketamine hydrochloride for blood drawing and 5-bromo-2′-deoxyuridine (BrdU) injection. BrdU was given i.v. or i.p. at schedules indicated in the figure legends.

Cell preparation and Ag stimulation

PBMC were isolated from heparinized or citrated venous blood by density gradient sedimentation using Ficoll-Hypaque (Histopaque-1077; Sigma-Aldrich, St. Louis, MO). Peripheral lymph node (PLN) and spleen cells were obtained by gentle mincing of tissues in complete medium (RPMI 1640 medium; HyClone Laboratories, Logan, UT) supplemented with 10% heat-inactivated FCS (HyClone Laboratories), 2 mM L-glutamine (Sigma-Aldrich), 1 mM sodium pyruvate (Sigma-Aldrich), and 50 μM 2-ME (Sigma-Aldrich) with splenocytes also subjected to Ficoll-Hypaque centrifugation to remove RBCs. Small intestinal lamina propria cells were obtained as previously described (24) from segments of small intestinal mucosa with as few grossly recognizable Peyer's patches as possible. Bronchoalveolar lavage cells were obtained by instilling and aspirating ~150 ml of PBS into the main bronchus of each lung at necropsy. All cells were washed twice in HBSS (Ca^{2+}/Mg^{2+}-free, Cellgro/Mediatech; Fisher Scientific, Federal Way, WA) and resuspended in complete medium.

Ag stimulations for intracellular cytokine staining were performed as follows: PBMC or other cell preparations were placed in polypropylene tissue culture tubes (BD Biosciences, Franklin Lakes, NJ) at 1×10^6 cells/ml complete medium (1–10 ml/tube) with appropriately titered "whole" RM CMV viral preparations (~50 μl of preparation/ml), CMV immediate early-1 (IE-1) 15-mer peptide mixes (Ref. 25 and see *Ags and Abs*), the superantigen staphylococcal enterotoxin B (SEB, 200 ng/ml; Toxin Technology, Sarasota, FL), or no Ag as a negative control (previously shown to be equivalent to mock virus preparations), with or without one or both of the costimulatory mAbs CD28 and CD49d (0.5 μg/ml each; these mAbs provide exogenous costimulation so as to allow the total cohort of Ag-specific cells to respond in this assay; Refs 26, 27). The cultures were routinely incubated at a 5° slant at 37°C in a humidified 5% CO_2 atmosphere for 6 h, with the final 5 h including 10 μg/ml brefeldin A (Sigma-Aldrich). After incubation, cells were harvested by washing in cold (4°C) Dulbecco's PBS (dPBS; Life Technologies, Rockville, MD) with 0.1% BSA (Roche Biochemicals, Indianapolis, IN) and were kept at 4°C until processed for staining.

Immunofluorescent staining and flow cytometric analysis

For cell surface staining, $0.25–1.0 \times 10^6$ cells were incubated with appropriately titered directly conjugated mAbs for 25 min at room temperature, followed by washing at 4°C, and resuspension in 1% paraformaldehyde in dPBS. Stained cells were then kept protected from light at 4°C until analysis on the flow cytometer. For intracellular cytokine analysis, stimulated cells were first stained on the cell surface with directly conjugated mAbs to CD3, CD4, CD8β, and other phenotyping markers (25 min each at room temperature), washed once with cold dPBS/BSA before resuspension in fixation/permeabilization solution (BD Biosciences, San Jose, CA; used at 2× recommended concentration) at 2×10^6 cells/ml, and incubated for 10 min at room temperature in the dark. Fixed and permeabilized cells were washed twice with cold dPBS/BSA, and then incubated on ice (protected from light) with directly conjugated anti-cytokine and CD69 mAbs for 25 min. Intracellular staining of Ki-67 vs cell surface markers was similar to cytokine analysis except that permeabilization was performed in 1× concentration fixation/permeabilization solution. For BrdU analysis (vs cell surface markers, Ki-67, or intracellular cytokine), cells were stained for surface markers first, fixed for 10 min at room temperature with FASCLyse solution (BD Biosciences), and then permeabilized for 12–14 h in 2× concentration fixation/permeabilization solution at 4°C. After washing twice with cold dPBS/BSA, cells were incubated on ice (protected from light) with directly conjugated mAbs specific for BrdU, Ki-67, anti-cytokine, and/or CD69 mAbs in the presence of 0.28 mg of bovine pancreas-derived DNase 1 (Sigma-Aldrich catalogue no. D4513) for 30 min. After staining, cells were resuspended in 1% paraformaldehyde in dPBS and stored in the dark at 4°C.

Six-parameter flow cytometric analysis was performed on a two-laser FACSCalibur instrument (BD Biosciences) using FITC, PE, peridinin chlorophyll protein-Cy5.5 (True Red), and allophycocyanin as the four-fluorescent parameters. List mode multiparameter data files (each file with forward scatter, orthogonal scatter, and four-fluorescent parameters) were analyzed by "cluster" analysis using the PAINT-A-GATE^{Plus} software program (BD Biosciences) (28). Special mention should be made of clustering $CD8^+$ T cells in RM. Whereas $CD4^+$ T cells can be accurately delineated by CD4 expression and small lymphocyte light scatter signals, this is not possible for $CD8^+$ T cells using conventional CD8α-specific reagents due to high expression of CD8α homodimers by RM NK cells and to low to moderate expression of these homodimers by $CD4^+CD28^-$ (effector memory) T cells (data not shown). Accurate clustering of conventional $CD8^+$ T cells (which express CD8$\alpha\beta$ heterodimers; data not shown) with a single fluorescence parameter therefore requires use of a CD8β-specific reagent (see below). The specificity of staining and criteria for determining positive staining for Ki-67 and BrdU were determined using isotype-matched negative control mAbs, and, in the case of BrdU, analysis of control (non-BrdU-pulsed) animals. The procedures and criteria for delineating and quantifying responding (CD69 positive/cytokine positive) vs nonresponding T cells have been previously described in detail (26, 27).

Ags and Abs

RM CMV (Cercopithecine Herpesvirus 8) Ag preparations were made from 68.1 strain (ATCC VR-677)-infected monolayers of primary RM fibroblasts after a 90–100% cytopathic effect was reached. Infected cells were scraped off the flasks, and then cells and media were clarified by centrifugation at $3840 \times g$ for 10 min. Cell pellets were resuspended in media, freeze-thawed three times, sonicated for 10 cycles (30 s/cycle), and then clarified by centrifugation at $3840 \times g$ for 10 min. Supernatants from both original culture media and lysed cell pellets were combined and the

[4] Abbreviations used in this paper: RM, rhesus macaque; BrdU, 5-bromo-2′-deoxyuridine; dPBS, Dulbecco's PBS; IE-1, immediate early-1; PLN, peripheral lymph node; MLN, mesenteric lymph node; SEB, staphylococcal enterotoxin B; int, intermediate.

virus was pelleted at 12,400 × *g* for 1 h. Viral pellets were resuspended in medium (2% of original culture volume) and titered in the cytokine flow cytometry response assay. RM CMV IE-1 peptides (consecutive 15-mers overlapping by 11 aa) were custom synthesized by Dr. D. Stoll (Natural and Medical Sciences Institute of the University of Tübingen, Tübingen, Germany) based on the IE-1 sequence of RM CMV strain 68.1 (GenBank accession no. M93360). Peptide sequences were confirmed by electrospray mass spectroscopy. To prepare total IE-1 mixes, the 137 overlapping peptides were individually solubilized in DMSO (Sigma-Aldrich) at 100 mg/ml and mixed together so that the final concentration of each individual peptide was 0.72 mg/ml. Two microliters of this mix was used per milliliter of cell stimulation medium (1.45 μg/ml final concentration of each peptide).

mAbs L200 (CD4; True Red, allophycocyanin conjugated), SP34 (CD3; FITC, PE, True Red, allophycocyanin), SK1 (CD8α; FITC, allophycocyanin), L78 (CD69; PE, allophycocyanin), L293 (CD28; unconjugated PE), CD28.2 (CD28; FITC), L25.3 (CD49d; unconjugated PE), L48 (Leu45RA; FITC), M-T271 (CD27; PE), G25.2 (CD11a; FITC), H111 (CD11a; PE), FIB504 (β_7 integrin; PE), SK11 (CD62L; PE), DX2 (CD95; allophycocyanin), B56 (Ki-67; FITC, PE), B44 (anti-BrdU; FITC), B27 (anti-IFN-γ; FITC, allophycocyanin), 11 (anti-TNF-α; FITC, allophycocyanin), and IgG1 and IgG2 isotype-matched controls were obtained from BD Biosciences. mAbs 2H4 (CD45RA; PE) and 2ST8.5h7 (CD8β; PE unconjugated) were obtained from Beckman Coulter (Fullerton, CA). Purified 2ST8.5h7 was custom conjugated to True Red by BD Biosciences.

Statistical analysis

Statistical analysis was conducted with the program Statview (Abacus Concepts, Berkeley, CA). The significance of differences between paired groups was analyzed with the Wilcoxon signed rank test. The relationships between variables were analyzed with the Spearman rank correlation test.

Results

Development of phenotypic criteria for naive/memory cell discrimination in RM

We adopted the following stepwise approach for the definition of naive and memory T cell subsets in RM: 1) assessment of mAbs known to delineate appropriate T cell populations in humans for (high-level) cross-reactivity with RM T cells, 2) selection of reagents and optimization of staining combinations so as to definitively separate the putative naive and memory populations and memory subsets of interest (e.g., the putative effector memory subset); and 3) validation of subset identity by functional analysis and studies of population dynamics. Our initial screening identified one or more mAbs against human CD11a, CD28, CD62L, CD45RA, CD49d, CD95, and β_7 integrin that were usefully cross-reactive with RM T cells and when assessed by multiparameter (four-color) flow cytometry in various combinations appeared to be capable of delineating putative naive and memory subsets (based on previous described criteria for human T cells (2, 4, 5, 18, 19)). Optimal separation of putative $CD4^+$ naive and memory T cells was achieved by the combination of CD95, β_7 integrin, and/or CD28 in which putative naive cells were apparent as a uniform $CD95^{low}CD28^{high}$, β_7 $integrin^{int}$ population (Fig. 1*A*). For $CD8^+$ T cells, CD95, CD28, and CD11a mAbs were the most discriminatory with the putative naive subset again showing the expected homogeneous phenotype—$CD95^{low}CD28^{int}CD11a^{low}$ (Fig. 1*B*).

These primary markers were then examined in various combinations with each other and with selected other markers (chosen for their ability to reproducibly subset the memory population) so as to confirm marker overlap and provide an extended phenotype of the putative naive and memory subsets. As illustrated in Fig. 1, putative naive T cells (both $CD4^+$ and $CD8^+$) comprise a phenotypically homogenous cluster of uniformly small cells (by light scatter criteria). The only exception to this phenotypic homogeneity was the frequent observation of variably sized subsets with apparent loss of CD62L intensity (likely due to the well-characterized propensity of this molecule to be down-regulated by proteolytic cleavage; Ref. 29). In contrast, putative memory cells were more variable in size (on average larger than naive cells) and demonstrated a strikingly phenotypic heterogeneity with variable expression of markers delineating multiple, clearly apparent subsets. Several general points are noteworthy. First, the commonly used "naive T cell" marker CD45RA appeared to be highly expressed by significant subsets of both $CD4^+$ and $CD8^+$ putative memory cells in RM. Second, $CD4^+$ and $CD8^+$ subsets were phenotypically analogous, but by no means identical, making separate analysis a requirement for accuracy. These differences included the relative intensity of various markers on particular subsets and the phenotypic configuration of the various memory subsets. Finally, some common patterns were discernible within the overall phenotypic heterogeneity of the memory population. The most notable pattern was the association of diminished or absent CD28 expression with relatively high CD11a, CD49d, and CD45RA, and relatively low CD62L and β_7 integrin expression among $CD4^+$ memory T cells (Fig. 1*A*, arrows). An analogous, but more complex, $CD28^-$ population was observed among $CD8^+$ cells. In addition to being substantially higher in frequency (see below), this subset showed more variable CD45RA expression and included a $CD11a^{dim}$, β_7 $integrin^{high}$ subset that was not present within the $CD4^+$ subset (Fig. 1*B*, arrows, and see next section below).

Validation of criteria for naive/memory cell discrimination in RM by subset localization and development

Extensive data in both rodents and humans have established that recirculation of naive T cells is largely, if not exclusively, restricted to secondary lymphoid tissues (PLN, spleen, Peyer's patch, tonsil), whereas memory cells are normally localized in both of these sites and extralymphoid "tertiary" sites (effector sites or potential effector sites) (5, 7, 30). In keeping with this paradigm, putative RM naive T cells, both $CD4^+$ and $CD8^+$, were essentially absent from representative tertiary sites (lung bronchoalveolar and small intestinal lamina propria T cells; Fig. 2), but formed a significant component of the T cell populations within PLN and spleen (Fig. 2 and Table I). As has been previously shown in other systems, small intestinal lamina propria memory cells (particularly the $CD8^+$ subset) were almost exclusively β_7 integrin positive, likely due to the role of $\alpha_4\beta_7$ integrin in mediating T cell homing to this site and to in situ up-regulation of $\alpha_e\beta_7$ integrin (7). $\alpha_4\beta_7$ integrin has not been implicated in lung T cell homing (31), and in this site the subset of β_7 $integrin^{int}$ cells apparent in Fig. 2 is predominantly due to in situ up-regulation of $\alpha_e\beta_7$ integrin (data not shown).

We also examined the question of whether peripheral blood frequencies of naive phenotype T cells reflect those of the various secondary lymphoid tissues. As shown in Table I, naive T cell frequencies in peripheral blood tended to underrepresent frequencies in PLN and mesenteric lymph nodes (MLN), slightly in the case of $CD4^+$ T cells (<15% on average) and more significantly in the case of $CD8^+$ T cells (22–26%). Strikingly, in the spleen, just the opposite was true; peripheral blood naive T cell frequencies were much higher than splenic frequencies, by a 2.5- to 3-fold ratio. This relative dearth of putative naive T cells (and excess of memory T cells) in the spleen might reflect the dual role of the spleen as a secondary lymphoid tissue (white pulp) and a potential effector site (red pulp) (5); the latter with an independent complement of memory T cells.

A second fundamental precept of the naive/memory paradigm is the dominance of the naive subset in the newborn and the subsequent development of the memory subset with postnatal Ag exposure (5). Again, the delineation of naive and memory subsets by

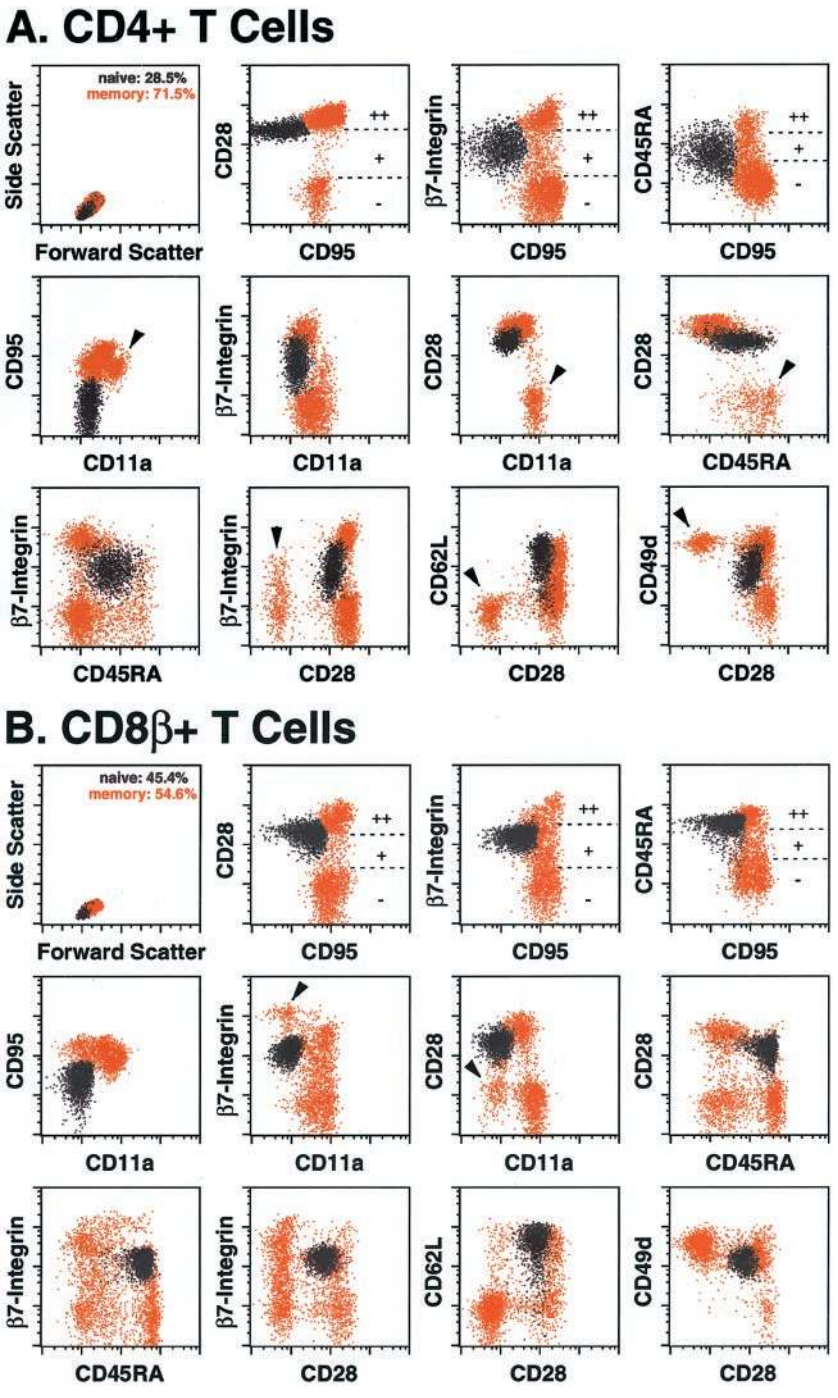

FIGURE 1. Coordinate expression of putative memory/naive markers on RM $CD4^+$ and $CD8^+$ T cells. RM PBMC (6.8-year-old animal) were examined for their correlated expression of cell surface CD4 or CD8β vs CD95 vs various paired combinations of CD28, CD45RA, CD11a, β_7 integrin, CD62L, and CD49d (α_4 integrin). Five thousand events gated on $CD4^+$ (*A*) or $CD8\beta^+$ (*B*) small lymphocytes are shown. The putative naive population is colored blue based upon characteristic homogeneous expression of these markers (2, 4), with the remaining cells (putative memory cells) colored red. Optimal discrimination of the naive cluster was observed with CD95 vs β_7 integrin vs CD28 for $CD4^+$ T cells and with CD95 vs CD28 vs CD11a for $CD8^+$ T cells, and the frequencies provided in the light scatter profiles reflect these combinations. However, the equivalency of the colored populations in each profile was tested by extensive cross-over analysis, and the coefficient of variation of the percent naive was <3% in these different analyses. The designations ++, +, and − reflect relative intensity levels of the indicated marker (using naive cell staining intensity as internal control) that define memory subsets referred to throughout this report. Arrowheads in *A* designate a distinct cluster of $CD28^-CD11a^{high}CD45RA^+CD62L^-$ cells, consistent with the $CD4^+$ T cell effector memory population (see text); arrowheads in *B* designate a unique subset of likely gut-associated $CD28^-CD8^+$ T cell effector memory cells characterized by bright β_7 integrin and dim CD11a.

the above criteria conforms well to this paradigm. As shown in Fig. 3, $CD4^+$ and $CD8^+$ lineage cells with a putative naive phenotype dominate in neonatal blood, but cells bearing a putative memory phenotype rapidly increase with postnatal age. Interestingly, unlike our published experience in humans (32, 33), small populations of memory T cells, particularly $CD8^+$ memory cells, are present in neonatal blood. Importantly, however, the frequency of these cells always increased with postnatal time, in keeping with our interpretation of these phenotypically defined subsets. It is also important to note that while memory T cells display defined β_7 integrin$^{high, int, and low}$ subsets at birth, few $CD28^-$ T cells are present in the neonatal memory population. This subset increases in relative frequency with postnatal time, consistent with a maturation process after the initial naive to memory transition (see below).

The frequency of memory T cells is known to increase progressively with age, as Ag encounters accumulate, and perhaps as thymic output of naive T cells declines (33). Cross-sectional analysis of 87 animals representing the life span of rhesus macaques demonstrates the close association of phenotypically defined peripheral blood memory T cell frequencies and age (Fig. 4). From these data, it appears that RM memory T cell development occurs very rapidly during childhood and adolescence and slows in adulthood. However, by old age (>20 years for RM), nearly all circulating T cells display a memory phenotype. Interestingly, $CD4^+$ and $CD8^+$ memory T cell frequencies are closely linked, perhaps reflecting a relationship between memory frequencies of both lineages and/or an independent association of these frequencies with an individual animal's cumulative exposure to T cell-stimulating Ag.

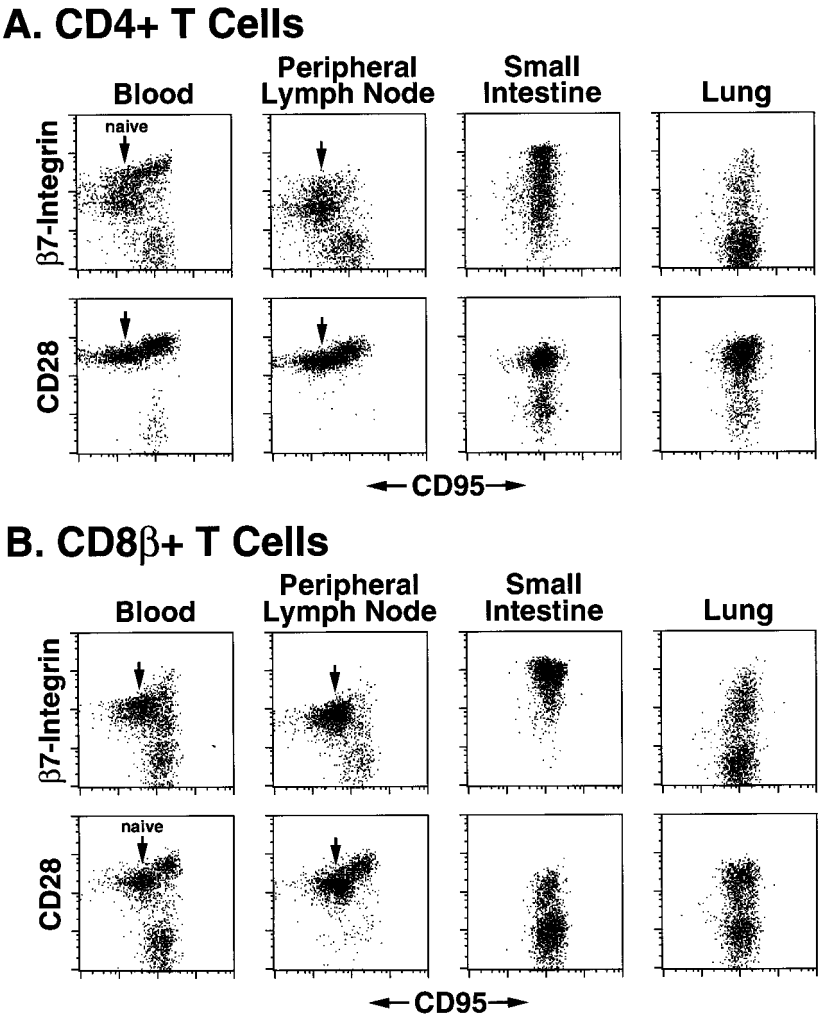

FIGURE 2. RM T cells bearing the putative naive phenotype are present in blood and secondary lymphoid tissue, but not extralymphoid effector sites. RM PBMC, and cells from PLN, small intestinal lamina propria, and bronchoalveolar lavage preparations (10.9-year-old animal) were examined for their correlated expression of cell surface CD4 or CD8β vs CD95 vs CD28 or β_7 integrin. Two thousand events gated on CD4$^+$ (*A*) or CD8β^+ (*B*) small lymphocytes are shown, with arrows designating the putative naive population in blood and PLN. Note the absence of a distinct naive T cell cluster in small intestine and lung.

Functional assessment of naive and memory T cell subsets

Perhaps the most fundamental differences between naive and memory T cells concern functional capabilities and TCR repertoire. With respect to the former, naive T cells are largely incapable of (immediate) synthesis of certain effector cytokines such as IFN-γ, even with optimal TCR stimulation and costimulation, whereas this capability is developed by memory T cells upon receiving appropriate differentiation signals during the naive to memory transition (34). With respect to repertoire, the naive subset manifests the broad thymic selected repertoire with clonal frequencies to any given (potential) Ag too low to be recognized by current functional assays without prior proliferative expansion (e.g., $\sim$1:10^6); in contrast, the memory subset manifests an Ag-selected repertoire and may include Ag-specific frequencies well above 1%,

Table I. *Frequency of naive T cells in peripheral blood vs lymphoid tissues*

		% Naive (blood:tissue ratio)[a]							
		CD4				CD8			
Animal	Age (years)	Blood	PLN[b]	MLN	Spleen	Blood	PLN	MLN	Spleen
16693	10.8	66.2	66.7 (0.99)	60.1 (1.10)	44.5 (1.49)	64.0	82.7 (0.77)	70.8 (0.90)	41.5 (1.54)
17892	7.1	56.7	49.0 (1.16)	71.8 (0.79)	16.9 (3.36)	53.8	62.7 (0.86)	72.3 (0.74)	12.0 (4.48)
20140	13.9	35.0	32.1 (1.09)	38.5 (0.91)	18.8 (1.86)	51.5	53.7 (0.96)	56.1 (0.92)	20.2 (2.55)
15007	13.9	40.3	35.2 (1.15)	55.9 (0.72)	13.0 (3.10)	47.4	46.1 (1.03)	61.9 (0.77)	16.1 (2.94)
18197	7.0	55.0	66.1 (0.83)	69.8 (0.79)	20.7 (2.66)	25.6	60.8 (0.42)	67.2 (0.38)	5.4 (4.74)
16297	10.9	50.6	53.4 (0.95)	55.6 (0.91)	29.9 (1.69)	42.4	72.4 (0.59)	66.3 (0.64)	22.1 (1.92)
15843	9.3	31.2	42.5 (0.73)	44.5 (0.70)	12.7 (2.46)	59.4	69.6 (0.85)	77.3 (0.77)	13.3 (4.47)
18468[c]	6.1	75.6	78.4 (0.96)	80.7 (0.94)	23.7 (3.19)	56.6	73.6 (0.77)	72.5 (0.78)	27.3 (2.07)
		Mean ratio	0.98	0.86	2.48		0.78	0.74	3.09

[a] Naive subset defined by CD95, CD28, and either β_7 integrin (CD4$^+$ T cells) or CD11a (CD8$^+$ T cells) expression as described in Fig. 1 legend.
[b] Inguinal and axillary.
[c] Attenuated SIV infected.

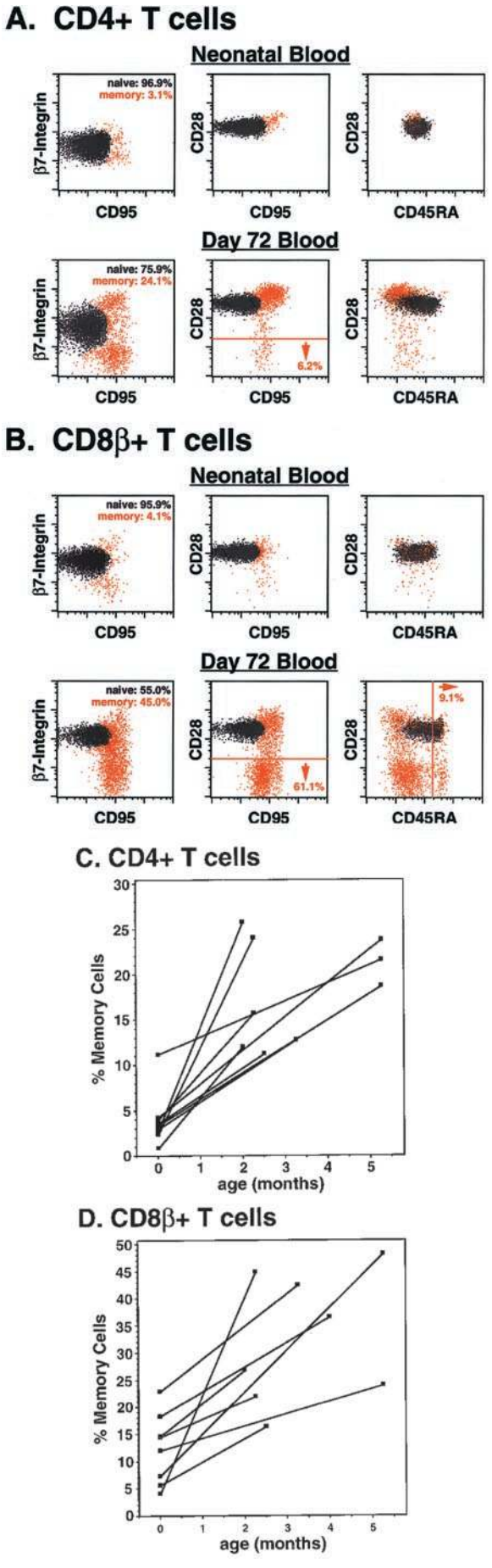

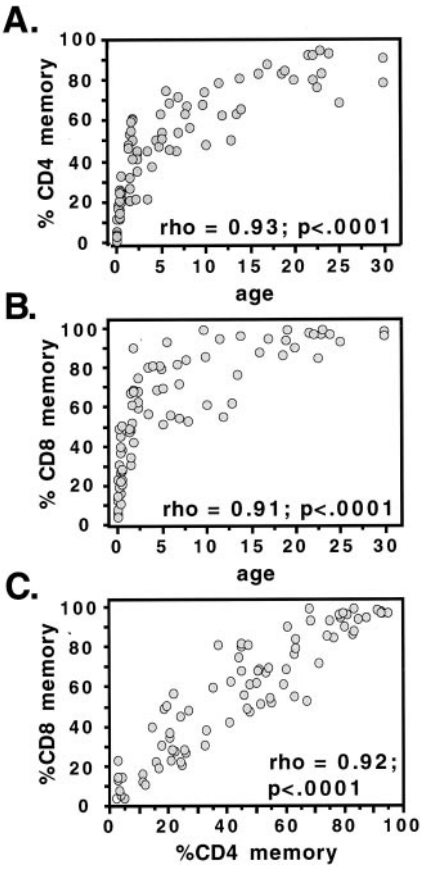

FIGURE 4. RM memory phenotype $CD4^+$ and $CD8^+$ T cells coordinately accumulate with age. This figure demonstrates a cross-sectional analysis of the frequencies of memory phenotype T cells throughout the RM life span. Memory T cell frequencies were determined using patterns of β_7 integrin, CD28, and CD95 expression, as shown in Figs. 1 and 3. Spearman rank correlation coefficients (ρ) and p values are shown for percent $CD4^+$ and percent $CD8^+$ memory T cell frequencies vs age and vs each other.

especially responses directed against persistent viruses like CMV (5). To test the functional and repertoire characteristics of our phenotypically defined subsets, we used cytokine flow cytometry, a technique that allows precise quantification and phenotypic characterization of TCR-triggered T cells (25–27). In this assay PBMC are incubated with Ag or other stimuli (and costimulatory Abs to lower response thresholds) for 6 h with the secretion inhibitor brefeldin A present the last 5 h. It is important to note that brefeldin A not only retains secreted products such as cytokines within the cell cytoplasm (in a modified Golgi), but also any induced cell

FIGURE 3. Peripheral blood T cells with a putative memory phenotype are rare at birth in RM, but rapidly accumulate in the first few months of postnatal life. PBMC from blood obtained in the first 24 h of life and at postnatal day 72 from the same RM were examined for their correlated expression of CD4 or CD8β vs CD95 vs CD45RA vs either CD28 or β_7 integrin and analyzed as described in Fig. 1 legend. Five thousand events gated on $CD4^+$ (*A*) or $CD8\beta^+$ (*B*) small lymphocytes are shown, with the overall percent naive (blue)/memory (red) provided in the top left profiles in each figure, and the percentage of the memory population with the designated phenotypes ($CD28^-$ or $CD45RA^{++}$) shown in association with defining lines and arrows. Similar analyses on sequential neonatal and 2- to 5-mo postnatal specimens were performed on seven additional RM, and the frequencies of $CD4^+$ (*C*) or $CD8\beta^+$ (*D*) T cells with the putative memory phenotype for all eight animals studied are shown.

surface molecules (27). Thus, even with potent polyclonal T cell stimulation, no change in surface phenotype (i.e., stained before fixation and permeabilization) is observed for most Ags during the course of this assay, including all those used as primary phenotyping markers in this study (data not shown).

To assess IFN-γ synthesis capabilities of putative naive vs memory subsets, we utilized stimulation with the superantigen SEB, which stimulates on the basis of TCR Vβ chain recognition (26), and thus stimulates both naive and memory subsets. To ensure suprathreshold stimulation of naive cells, we also included costimulatory mAbs (either CD28 and CD49d or CD49d alone). As illustrated in Fig. 5 (representative of five independent experiments with different animals), this stimulation protocol elicited substantial frequencies of IFN-γ-producing cells in both the $CD4^+$ and $CD8^+$ subsets—responses that were restricted almost entirely to the phenotypically defined memory population. This restriction was similar regardless of the level of exogenous costimulation provided (none, CD49d alone, or CD28 plus CD49d; data not shown). Importantly, IFN-γ producers were well represented in all β_7 integrin-, CD28-, and CD45RA-defined memory subsets, although the frequency of such responders in these subsets varied among different animals (likely due to different distributions of T cells with appropriate TCR-Vβ).

To determine the phenotype of memory T cells defined by the capacity to manifest an immediate effector response to recall Ag, we examined the $CD4^+$ T cell response to whole RM CMV preparations, and the $CD8^+$ T cell response to a set of consecutive 15-mer peptides (overlapping by 11 aa) representing the sequence of RM CMV *IE-1* gene (which contains at least 6 dominant class I-restricted T cell epitopes recognized by RM in our colony; J. Walker and L. Picker, manuscript in preparation). As illustrated in Fig. 6 (representative of four animals), both RM CMV-specific $CD4^+$ T cells and RM CMV IE-1-specific $CD8^+$ T cells were highly restricted to the putative memory subset (again, this restriction was observed regardless of the level of exogenous costimulation; data not shown). Interestingly, in the case of these responses to a persistent virus, the responding cells were not equivalently distributed among all memory subsets (Table II). RM CMV-specific $CD4^+$ memory cells were predominantly $CD28^{-\text{ to dim}}$, β_7 integrin$^{-\text{ to dim}}$, and $CD45RA^{+\text{ to }++}$. Among the animals tested, an average of 81% of the $CD4^+$ T cell response to CMV was composed of $CD28^{-\text{ to dim}}$ memory cells, whereas the overall frequency of $CD28^{-\text{ to dim}}$ cells in the same samples was 11.5% (7-fold enrichment). IE-1-specific $CD8^+$ T cells were similarly polarized with respect to β_7 integrin and CD45RA, but were much more polarized with respect to CD28: >95% of these cells lacked or showed dim expression of CD28 (although due to the high overall frequency of $CD28^{-\text{ to dim}}$ memory cells in the $CD8^+$ T cell subset of these animals (52%), the overall enrichment was only ~2-fold).

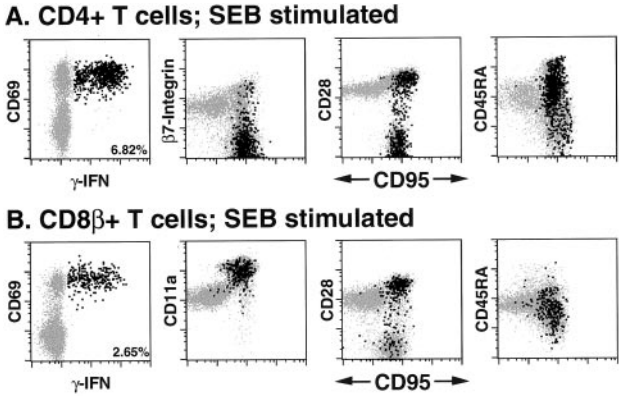

FIGURE 5. Memory, but not naive, phenotype T cells produce IFN-γ after superantigen stimulation. RM PBMC (8.4-year-old animal) were stimulated with the superantigen SEB plus CD49d for 6 h in the presence of the secretion inhibitor brefeldin A for the final 5 h, and then examined for their correlated expression of cell surface CD4 or CD8β vs CD95 vs either β_7 integrin, CD28, CD45RA, or CD11a (stained before fixation and permeabilization) vs intracellular IFN-γ (stained after fixation and permeabilization), or cell surface CD4 or CD8β vs intracellular IFN-γ and CD69. Ten thousand events gated on $CD4^+$ (*A*) or $CD8\beta^+$ (*B*) small lymphocytes are shown, with the events within the IFN-γ^+ (SEB-responding) population enlarged and colored black (percent responding provided in the lower right corner of the CD69 vs IFN-γ profile). Parallel cultures treated with CD49 mAbs alone and analyzed in similar fashion revealed no IFN-γ response (data not shown).

Identification of RM effector memory T cells

Although the concept of specific functional specialization among memory T cells goes back many years, there has been recent appreciation for a broad dichotomy in memory T cell differentiation based on the ability of a memory cell to manifest immediate (i.e., without further maturation), direct anti-pathogen effector activities in tertiary (extralymphoid) sites (8, 18, 22, 23, 30, 35–44). So-called effector memory T cells are thought to be fully, perhaps terminally, differentiated cells with high potential for immediate cytotoxic function, polarized cytokine synthesis function (e.g., Th1 vs Th2), predominant homing to and localization within extralymphoid tissues, and reduced costimulatory requirements. This population also includes the majority of memory T cells specific for chronic pathogens, and accumulates with age. Effector memory T cells are thought to derive from so-called "central" memory cells which have little immediate cytotoxic potential, nonpolarized cytokine synthesis function, predominant homing to and localization within secondary lymphoid tissues, and higher costimulatory requirements. Although the phenotypic correlates used to delineate these populations vary among investigators, CD27, CD28, CD45RA, CCR7, and CD62L have been the most widely used in humans, with the most differentiated effector memory population characterized as $CD27^-$, $CD28^-$, $CD45RA^+$, $CCR7^-$, and $CD62L^-$, and the "archetype" central memory population having the reciprocal phenotype.

As indicated above, analogous $CD28^-$ and $CD45RA^{high}$ memory subsets were recognizable, indeed quite prominent, in the RM, and included most of the RM CMV-specific memory T cells in both the $CD4^+$ and $CD8^+$ lineages. To further evaluate the significance of these phenotypes, we quantified the frequencies of the $CD28^-$ and $CD45RA^{high}$ subsets within the overall population of peripheral blood memory cells in our cross-sectional cohort of 87 animals and correlated these frequencies with age and with each other. As shown in Fig. 7, there was a striking correlation between the size of the $CD28^-$ subset and age for both the $CD4^+$ and $CD8^+$ populations, although the pattern of this relationship was different for the two lineages. The fraction of memory $CD8^+$ T cells with a $CD28^-$ phenotype rapidly increased in the first 3 years of life and then leveled off; whereas for $CD4^+$ memory cells, the accumulation of $CD28^-$ cells was more gradual and continued through adulthood. For the $CD4^+$ lineage, the $CD45RA^{high}$ subset showed a similar correlation with age and, in fact, demonstrated a strong, direct correlation with the $CD28^-$ subset (in keeping with our general impression on multiparameter flow cytometric analysis that in peripheral blood, these two subsets were largely, although not completely, overlapping; Fig. 1*A* and data not shown). In contrast, the $CD8^+$/$CD45RA^{high}$ memory subset showed no correlation with age or with the $CD8^+CD28^-$ subset. Indeed, multiparameter analysis of these two markers on $CD8^+$ memory cells

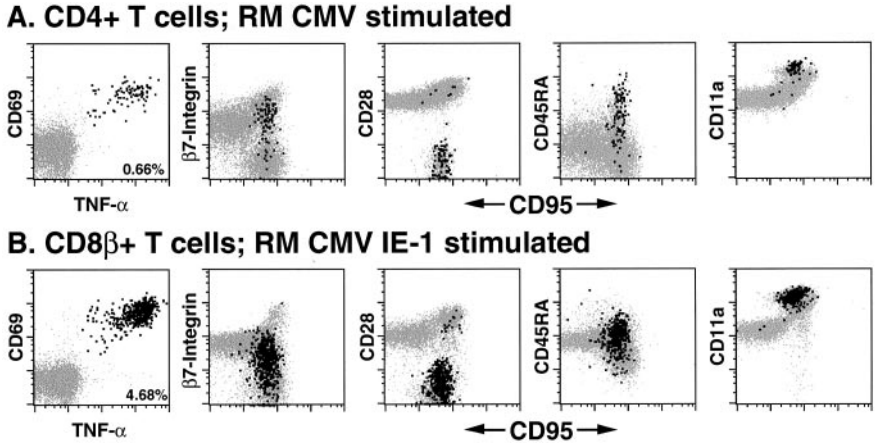

FIGURE 6. T cells responding to the chronic virus RM CMV display a memory phenotype. RM PBMC (9.5- and 8.4-year-old animals for *A* and *B*, respectively) were stimulated with the whole CMV Ag preparations ($CD4^+$ T cells; *A*) or IE-1 peptide mixes (consecutive 15-mers overlapping by 11 aa; $CD8^+$ T cells, *B*) plus CD49d for 6 h in the presence of the secretion inhibitor brefeldin A for the final 5 h, and then examined for their correlated expression of cell surface CD4 or CD8β vs CD95 vs either β_7 integrin, CD28, CD45RA, or CD11a (stained before fixation and permeabilization) vs intracellular TNF-α (stained after fixation and permeabilization), or cell surface CD4 or CD8β vs intracellular IFN-γ and CD69. Fifteen thousand events gated on $CD4^+$ (*A*) or $CD8\beta^+$ (*B*) small lymphocytes are shown, with the events within the TNF-α plus (Ag-responding) population enlarged and colored black (percent responding provided in the lower right corner of the CD69 vs IFN-γ profile; see also Table II). Parallel cultures treated with CD49 mAbs alone and analyzed in similar fashion revealed no IFN-γ response (data not shown).

revealed multiple nonoverlapping patterns of expression (Fig. 8*A*). Furthermore, whereas $CD8^+CD28^-$ memory cells were highly enriched in effector sites (lung and gut lamina propria) as compared with lymph node, $CD8^+CD45RA^{high}$ memory cells were highest in peripheral blood, next highest in lymph node, and almost absent in the effector sites examined (Fig. 8*B*). This same relative tissue distribution was observed for $CD4^+CD28^-$ and $CD4^+CD45RA^{high}$ T cells as well (data not shown), suggesting that the correlation of the $CD28^-$ and $CD45RA^{high}$ phenotypes observed in the $CD4^+$ memory T cell subset in peripheral blood did not extend to $CD4^+$ memory T cells in tissues. Taken together, these data support the conclusion that the $CD28^-$ phenotype consistently delineates RM effector memory differentiation for both $CD4^+$ and $CD8^+$ T cells, whereas the $CD45RA^{high}$ phenotype does not.

In vivo homeostasis of naive and memory subsets

Data in both rodent models and humans have indicated that homeostasis of naive and memory cells is achieved by fundamentally different mechanisms: naive T cells are thought to be long-lived, with only low-level homeostatic turnover, whereas memory T cell homeostasis is associated with high turnover (9, 20, 45). To investigate the in vivo turnover of the phenotypically defined subsets described above, we used two complementary approaches: 1) in vivo pulsing with the thymidine analog BrdU followed by quantification of $BrdU^+$ T cells, and 2) quantification of T cells expressing the cell cycle-associated nuclear Ag Ki-67. BrdU incorporation allows precise determination of cells in S phase during the pulse, and labeled cells can be followed over time. Staining is very discrete, and thus it is precisely quantitative. The main liability of this approach is the potential toxicity of BrdU (Ref. 46; although doses used here had no discernible toxic effects) and the impracticality of its use in large RM cohorts.

In contrast, Ki-67 reactivity, which implies a cell is cycling (i.e., non-G_o phase; Ref. 47), requires no pretreatment of the animals, and thus can readily be applied to large cohorts. However, Ki-67 expression is less discrete than that of BrdU, and its expression may miss cells proliferating in tissues that return to G_o phase before returning to peripheral blood. Moreover, the temporal significance of Ki-67 expression in vivo is poorly characterized; i.e., it is unclear whether Ki-67 reactivity suggests that a cell that has undergone DNA synthesis in the last few hours, the last few days, or even more remotely. To better interpret the in vivo significance

Table II. *Distribution of CMV-specific T cells within the memory subsets defined by CD28, CD45RA, and β_7 integrin*

Animal	Age (years)	Stimulus[a]	Responder Frequency (%)	% of Response within Memory Subsets								
				CD28			CD45RA			β_7 integrin		
				−	+	++	−	+	++	−	+	++
$CD4^+$ T cells												
16604	9.3	CMV alone	0.30	54.7	26.7	11.9	21.0	35.5	39.5	69.4	23.8	2.9
16242	10.6	CMV alone	0.60	51.9	22.5	21.5	27.0	18.0	50.8	75.3	14.6	6.1
16476	9.5	CMV + CD49d	0.66	84.6	3.6	10.2	13.2	51.5	33.8	12.1	56.3	30.0
15817	11.8	CMV + CD49d	0.47	77.1	1.5	18.8	24.5	34.2	38.4	29.4	51.9	14.5
$CD8^+$ T cells												
16604	9.3	IE-1 + CD49d	5.12	99.0	0.6	0.1	7.0	61.5	30.9	24.7	71.6	3.4
16476	9.5	IE-1 + CD49d	1.14	85.3	10.1	3.0	48.8	39.2	10.4	3.4	81.2	13.8
20096	8.4	IE-1 + CD49d	4.73	95.1	1.3	2.7	24.6	57.6	16.9	31.4	66.4	1.3
17180	8.9	IE-1 + CD49d	5.32	93.2	3.4	1.0	19.1	67.2	11.2	17.2	69.6	10.7

[a] CMV, Whole rhesus CMV preparations; IE-1, total mix of rhesus CMV IE-1 15 mer peptides (11 aa overlap).

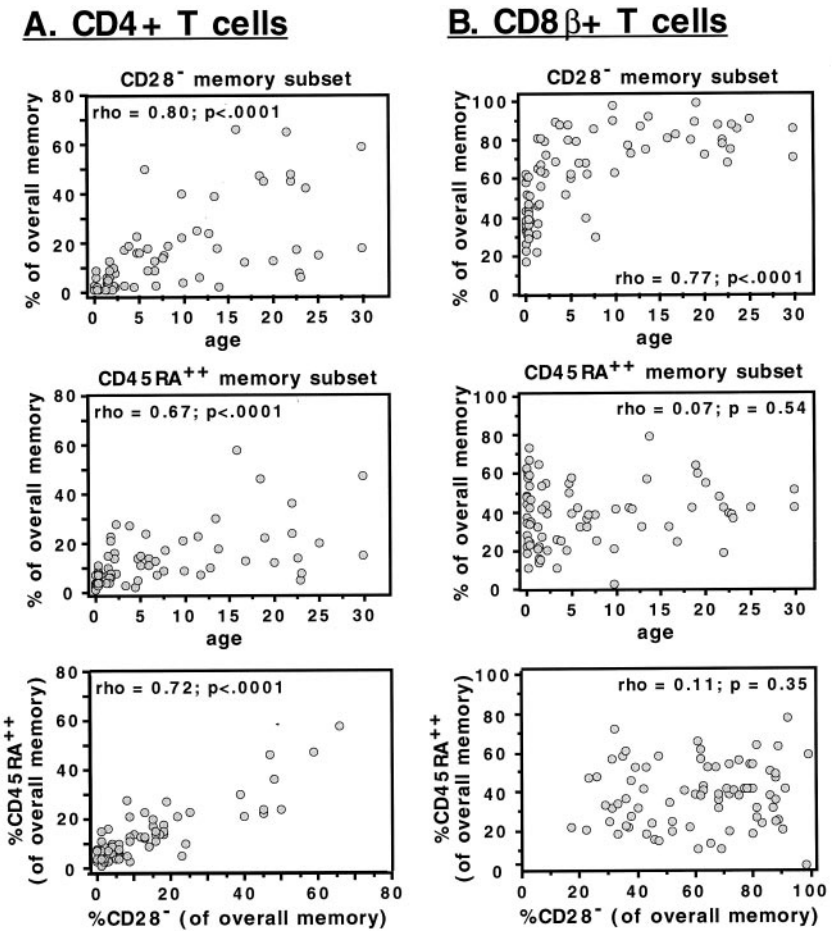

FIGURE 7. Frequencies of $CD28^-$ T cells in peripheral blood increase with age within both the $CD4^+$ and $CD8^+$ memory T cell subsets, whereas $CD45RA^{++}$ cells accumulate with age only within the $CD4^+$ memory subset. This figure demonstrates a cross-sectional analysis of the frequencies of $CD28^-$, $CD45RA^{++}$, $CD4^+$, or $CD8\beta^+$ T cells within the overall memory phenotype T cell population vs age of the animal and each other. $CD28^-$ and $CD45RA^{++}$ memory T cell frequencies were determined as shown in Fig. 1. Spearman rank correlation coefficients (ρ) and p values are shown for each analysis.

of Ki-67 reactivity in RM, we focused our initial experiments on the coordinate study of Ki-67 and BrdU expression by T cells harvested immediately after varying periods of in vivo BrdU exposure in different animals. As shown in Fig. 9*A* for $CD4^+$ T cells, 1 h after a single i.v. dose of BrdU, few Ki-67^+ cells are also $BrdU^+$. After three i.v. doses of BrdU over 24 h, only ~31% of Ki-67^+ cells are $BrdU^+$. However, after two i.v. doses a day of BrdU for 3 consecutive days, 75% of total Ki-67^+ and essentially all Ki-67^{bright} cells are $BrdU^+$; in addition, there are few $BrdU^+$ cells that lack Ki-67. After administering single high i.p. doses of BrdU for 4 consecutive days (given i.p. to prolong drug availability), essentially all Ki-67^+ are $BrdU^+$, but in this situation many of the $BrdU^+$ cells (~30%) are clearly beginning to lose Ki-67 reactivity. These observations suggest that Ki-67 expression delineates cells that have undergone S phase in the prior 3–4 days, and that few, if any, T cells in these normal animals remain arrested in the G_1 phase of the cell cycle (e.g., remain Ki-67^+ without going through S phase and becoming $BrdU^+$) for longer than this time period.

The fate of Ki-67 expression on the BrdU-labeled $CD4^+$ T cells is shown for the 3-day BrdU-pulsed animal (animal 15463) in Fig. 9*B*. Note that the vast majority of $BrdU^+$ cells lose Ki-67 reactivity by 1 wk following the end of the BrdU pulse. At 2 or more weeks after the BrdU pulse, the frequency of BrdU-labeled cells that also express Ki-67 remains steady at 2–6%, similar to the Ki-67 reactivity of the unlabeled population (data not shown). These results suggest that 1) few cells arrest in the G_2-M phase of the cell cycle (e.g., remain $BrdU^+$ without eventually leaving the cell cycle and losing Ki-67 reactivity), and 2) the vast majority of recirculating peripheral T cells undergo short bursts of expansion and then return to a noncycling state. The small fraction of $BrdU^+$ cells that express Ki-67 after week 2 likely represent stochastic re-entry of cells into the cell cycle, rather than continuous cell cycling, as continuous proliferation in the absence of exogenous BrdU would result in the loss of detectable BrdU reactivity after approximately four or five divisions. The results shown in Fig. 9 are for $CD4^+$ T cells, but essentially identical staining patterns were observed for the $CD8^+$ lineage of this animal and for both $CD4^+$ and $CD8^+$ T cells of a 6-day BrdU-pulsed animal (animal 15449; data not shown).

We next determined the recent proliferative history of putative naive and memory RM T cells by assessment of the correlated expression of either CD4 or CD8β, Ki-67, CD95, and in separate analyses β_7 integrin or CD28 by multiparameter flow cytometry. As illustrated in Fig. 10, *A–C*, and shown for 25 animals in Fig. 10*D*, frequencies of Ki-67^+ cells were ~10-fold higher in the memory than in the naive subset. Interestingly, for both the memory and naive subsets, Ki-67^+ frequencies within the $CD4^+$ and $CD8^+$ were highly correlated (Fig. 10*D*), indicating that within individual animals, homeostatic mechanisms, or in the case of memory cells, Ag encounters tend to coordinately impact both of these subsets. It was also of particular interest to assess the relative proliferative activity of memory subsets defined by CD28. As shown in Fig. 11, no significant difference in Ki-67 frequencies between the $CD28^{high}$ and $CD28^{low}$ memory subsets were observed for either the $CD4^+$ or $CD8^+$ populations. Thus, recent proliferative activity does not appear to distinguish effector and central memory populations.

Although studied in fewer animals, assessment of BrdU incorporation immediately after 1 day ($n = 2$), 3 days ($n = 1$), 4 days

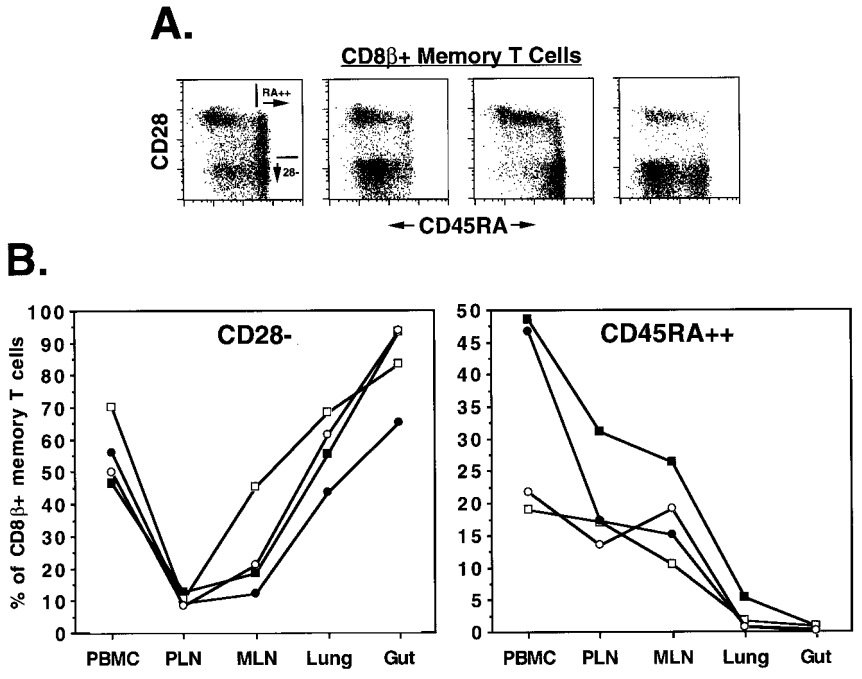

FIGURE 8. The $CD8^+CD28^-$ and $CD8^+CD45RA^{++}$ memory subsets are divergent with only the $CD28^-$ subset showing enrichment in effector sites. *A,* RM PBMC from four different animals (0.4, 3.4, 5.0, and 9.8 years old from left to right, respectively) were examined for their correlated expression of cell surface CD8β vs CD95 vs CD28 vs CD45RA. Five thousand events gated on $CD8\beta^+CD95^{high}$ (memory) small lymphocytes are shown. These profiles represent the spectrum of patterns observed for expression of CD28 and CD45RA among $CD8^+$ memory T cells; note the lack of correspondence of the $CD28^-$ and $CD45RA^{++}$ subsets. *B,* $CD8^+CD28^-$ and $CD8^+CD45RA^{++}$ memory subsets were defined as indicated in Figs. 1*B* and 8*A* and quantified in four different animals (□, 7.0 years old; ■, 12.3 years old; ○, 9.1 years old; ●, 10.9 years old) in PBMC, PLN, MLN, bronchoalveolar lavage cells (lung), and small intestinal lamina propria cells (gut).

($n = 1$), and 6 days ($n = 2$) of BrdU administration confirmed the subset distribution of proliferating T cells, particularly the proliferative competence of the $CD28^-$ effector memory population (Fig. 12 and data not shown). To further assess the proliferative capacity and survival of effector vs central memory cells, we followed the fate of BrdU-labeled total memory, $CD28^-$ and $CD28^+$ memory, and CMV-specific memory T cells over time in two of these animals. As shown in Fig. 12*A*, the rate of loss of $BrdU^+$ total memory T cells was highest in the first 1–2 wk after the pulse and then leveled off. Most significantly, loss of BrdU-labeled cells from the $CD28^-CD4^+$ and $CD28^-CD8^+$ memory subsets was similar to the loss of $BrdU^+$ cells in the corresponding $CD28^+$ subsets. In addition, the spectrum of BrdU intensities among the $BrdU^+$ cells was similar for both the $CD28^+$ and $CD28^-$ memory subsets, with neither population demonstrating a discernible shift to lower intensities at later time points (Fig. 12*B*). Loss of $BrdU^+$ cells in a given subset could result from 1) death of the labeled cells, 2) phenotypic differentiation of the labeled cells (e.g., $CD28^+$ memory cells converting to the $CD28^-$ subset), or 3) continued proliferation of the labeled cells, the latter being first recognized by loss of BrdU intensity, before such loss results in the inability to distinguish label. Thus, these observations would suggest that either the $CD28^-$ effector memory subset is equivalently stable as the $CD28^+$ central memory subset (i.e., with similar fractions of cells surviving without significant proliferation), or that a more rapid loss of labeled cells in the $CD28^-$ effector memory subset is largely compensated by the continued differentiation of ($BrdU^+$) $CD28^+$ precursors. Since the relative BrdU staining intensity of $CD28^-$ memory cells is stable, even at later time points, any such differentiation would have to occur in the absence of significant proliferation of these precursors and would imply a large reservoir of such cells in lymphoid tissues. Although this

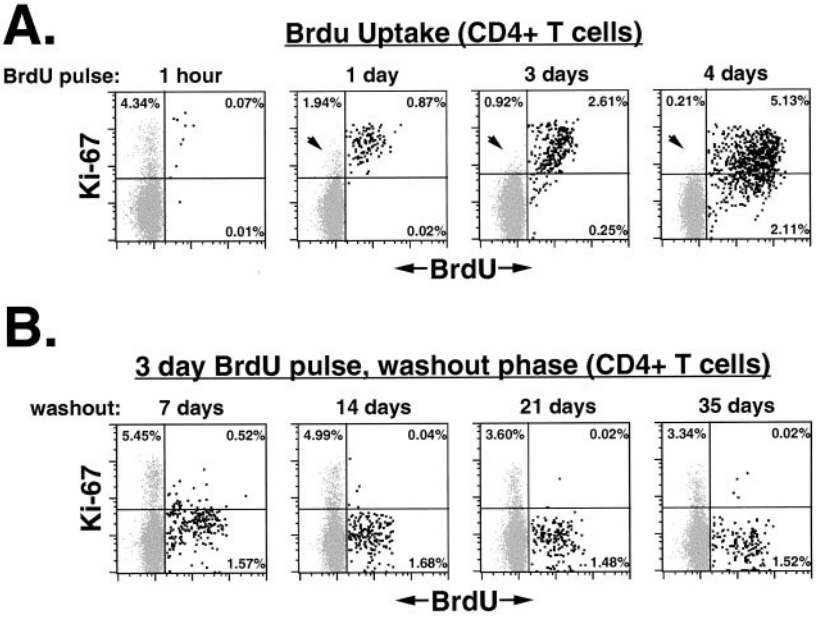

FIGURE 9. Ki-67^+ reactivity delineates T cells that have undergone S phase in the preceding 3–4 days, and when analyzed in conjunction with BrdU pulsing allow estimation of T cell turnover. *A,* Different RM were i.v. pulsed with BrdU for 1 h (100-mg single i.v. dose, PBMC collected 1 h later), 1 day (three 100-mg i.v. doses, given 8 h apart with PBMC collection 2 h after the last dose), 3 days (two 150-mg i.v. doses/day for 3 days with PBMC collection 14 h after last dose), or 4 days (single 700-mg i.p. dose/day for 4 days with PBMC collection 21 h after last dose). PBMC were examined for their correlated expression of cell surface CD4 vs CD8β vs intracellular BrdU and Ki-67. Ten thousand events gated on $CD4^+$ small lymphocytes are shown. *B,* The 3-day pulsed animal shown in *A* was followed at the designated intervals with the same analysis. Again, 10,000 events, gated on $CD4^+$ small lymphocytes, are shown. Identical patterns were seen for $CD8^+$ T cells in this animal and for both $CD4^+$ and $CD8^+$ T cells in an additional animal pulsed with BrdU at 150 mg i.v. for 6 days and studied at the same time intervals.

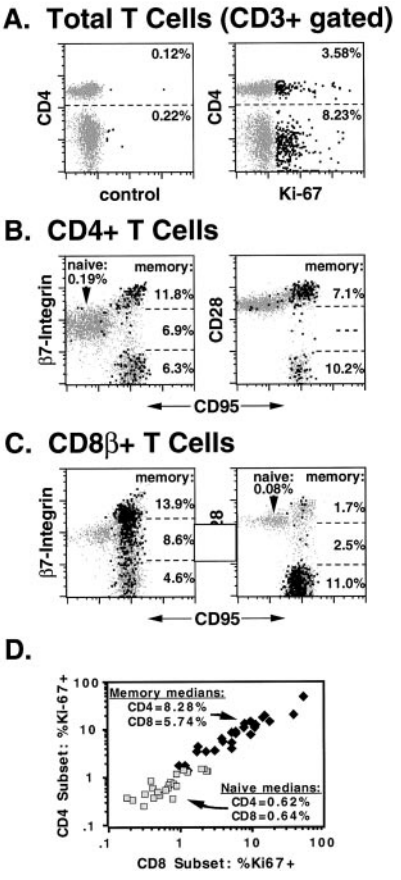

FIGURE 10. RM memory phenotype $CD4^+$ and $CD8^+$ T cells display markedly higher recent proliferative activity than their naive phenotype counterparts. RM PBMC (3.8-year-old animal) were examined for their correlated expression of cell surface CD3 vs CD4 vs CD8β vs intracellular Ki-67 (*A*), cell surface CD4 vs CD95 vs either β_7 integrin or CD28 vs intracellular Ki-67 (*B*), and cell surface CD8β vs CD95 vs either β_7 integrin or CD28 vs intracellular Ki-67 (*C*). Five thousand events gated on $CD3^+$ (*A*), $CD4^+$ (*B*), or $CD8\beta^+$ (*C*) small lymphocytes are shown, with the events within the control$^+$ (*A, left panel*) or $Ki\text{-}67^+$ population (*A, right panel*; *B* and *C*) enlarged and colored black (percent positive provided in each profile for the designated subsets). In *A*, it should be noted that the $CD3^+CD4^-$ subset shown is equivalent to the $CD3^+CD8\beta^+$ population. *D,* Cross-sectional analysis of the frequencies of $Ki\text{-}67^+$ cells (shown on a log scale) within the naive (▨) and memory (♦) subsets of the $CD4^+$ vs $CD8\beta^+$ T cell populations in the peripheral blood of 25 RM (age range, 1.4–12.6 years). $Ki\text{-}67^+$ cell frequencies within these subsets were determined on the CD95 vs β_7 integrin profiles for the $CD4^+$ subset and the CD95 vs CD28 profiles for the $CD8\beta^+$ subset. Spearman rank correlation coefficients (ρ) and p values for $CD4^+$ vs $CD8^+$ naive and $CD4^+$ vs $CD8^+$ memory $Ki\text{-}67^+$ frequencies are $\rho = 0.82$; $p < 0.0001$ and $\rho = 0.92$, $p < 0.0001$, respectively.

might be plausible for the overall memory subset, our analyses have indicated that the CMV IE-1-specific $CD8^+$ memory cohort is predominantly $CD28^{-\text{ to low}}$ throughout the body (extrapolated over blood, spleen, secondary lymphoid tissues—PLN and spleen, and effector sites—lung; Fig. 5, Table II, and data not shown). Thus, the demonstration that the IE-1-specific population has, if anything, a slightly slower rate of $BrdU^+$ cell loss than the overall $CD28^-$ subset (Fig. 12) argues against the possibility that $BrdU^+$ cell frequencies are maintained in the effector memory subset by continual replacement from a central memory reservoir.

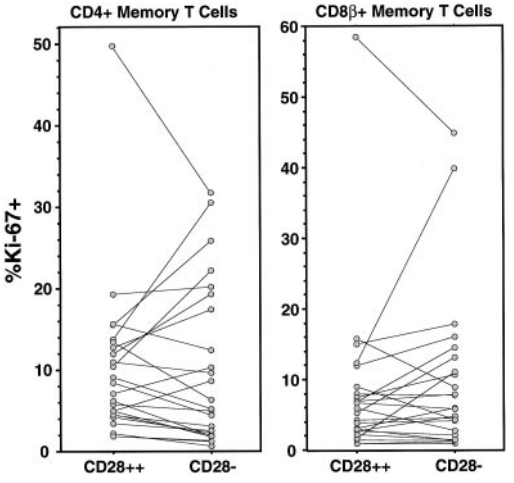

FIGURE 11. $CD28^-$ effector memory and $CD28^{++}$ central memory T cell subsets cannot be distinguished on the basis of recent proliferative activity. This figure demonstrates a cross-sectional analysis of the frequencies of $Ki\text{-}67^+$ cells within the CD28-defined memory subsets (see Fig. 1) of the $CD4^+$ vs $CD8\beta^+$ T cell populations in the peripheral blood of the same cohort used in Fig. 10*D*. Statistical analysis (Wilcoxon signed rank test) demonstrated no significant difference between $Ki\text{-}67^+$ cell frequencies of the $CD28^{++}$ and $CD28^-$ memory subsets for either the $CD4^+$ or $CD8^+$ T cell populations ($p = 0.67$ and 0.39, respectively).

Discussion

In this study, we have adapted the latest technologies in phenotypic and functional cellular analysis to the study of T cell memory in a nonhuman primate model. Our primary goals were 2-fold. First, we wanted to bring the study of RM T cell memory to current levels of understanding in the human system, essentially creating a data set in one study that recapitulates and refines an ~14-year evolution of data and concepts from disparate human studies. The main aim of this part of the study was to rigorously correlate cell surface marker expression and function among RM T cells so as to phenotypically and functionally define naive/memory status and physiologically relevant memory subsets in this model. Such information is critically needed to support ongoing studies using the RM as an infectious disease and vaccine model (SIV, among others) and to allow the exploitation of this model for fundamental investigations of primate memory T cell physiology. The second goal involved the initiation of these later investigations, developing approaches to examine the homeostasis of RM memory T cell populations, and then to test basic concepts of such homeostasis in vivo.

With regard to validating phenotypic signatures of naive vs memory status, we have developed an analysis paradigm that clearly delineates, for both the $CD4^+$ and $CD8^+$ T cells, distinct populations with the expected physiologic characteristics of these subsets (4, 5, 7–10). As summarized in Table III, the homogenous naive cell cluster, best delineated as $CD95^{low}$, B_7 $integrin^{int}$, and $CD28^{high}$ among $CD4^+$ T cells and by $CD95^{low}$, $CD28^{int}$, and $CD11a^{low}$ among $CD8^+$ T cells, was 1) present in blood and secondary lymph tissues (PLN, spleen), but not effector sites (lung, intestinal lamina propria); 2) vastly predominated in the fetal/neonatal immune system, but rapidly diminished with postnatal age; 3) lacked IFN-γ production capability and specific responses to RM CMV; and 4) demonstrated low in vivo proliferative activity/turnover. Most previous studies analyzing naive T cells in RM have relied upon CD45RA expression alone or the combination of CD45RA expression and CD62L expression to delineate this subset (48–51). When other markers (CD11a, CD28, CD49d, CD95)

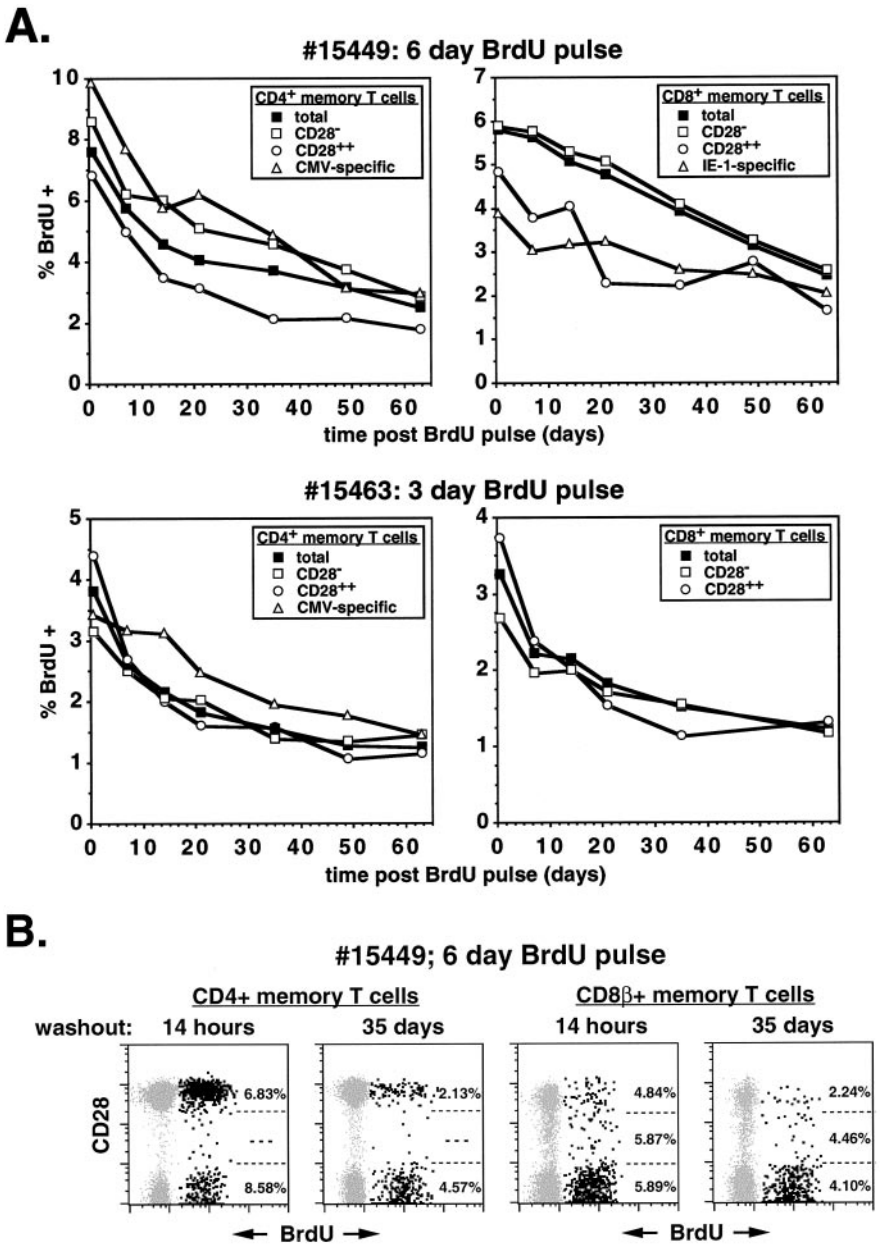

FIGURE 12. BrdU-labeled memory T cell populations defined by high or low expression of CD28 and by specificity for CMV determinants show a similar rate of decay after BrdU washout. *A,* RM 15449 (13.0 years old) and RM 15463 (13.2 years old) were i.v. pulsed with BrdU for 6 days (single 150-mg dose of BrdU/day) and 3 days (150-mg of BrdU twice a day), respectively, and PBMC were harvested at 14 h and 7, 14, 21, 35, 49, and 63 days after the last dose. Fresh PBMC were examined for their correlated expression of cell surface CD4 or CD8β vs CD95 vs CD28 vs intracellular BrdU. Separate aliquots were stimulated with CMV Ag or IE-1 peptide mix as described in Fig. 5 legend and were then stained for cell surface CD4 and CD3 and intracellular TNF-α, and BrdU (RM 15449; the $CD3^+CD4^-$ phenotype was used to define the $CD8^+$ T cell response to IE-1), or surface CD4 and intracellular CD69, TNF-α, and BrdU (RM 15463). Frequencies of $BrdU^+$ were determined in the total, $CD28^{++}CD28^-$, CMV/IE-1-responsive (TNF-α^+) $CD4^+$ and $CD8^+$ memory subsets. *B,* Representative flow cytometric profiles of the analysis in *A* (animal 15449). Ten thousand events gated on $CD4^+CD95^{high}$ or $CD8\beta^+CD95^{high}$ (memory) small lymphocytes are shown. $BrdU^+$ events are enlarged and colored black, with the percent $BrdU^+$ for the $CD28^{++}$, $CD28^+$, and $CD28^-$ memory subsets indicated in each panel (except for the $CD4^+CD28^+$ subset, where cells were too few for accurate analysis). Note that although the frequency of $BrdU^+$ T cells diminished over the 35-day period shown (most profoundly for the $CD28^{++}$ subset), there is no discernible difference in the spectrum of BrdU staining intensities between the 14-h and 35-day samples for any of the subsets shown.

have been used for phenotyping RM T cells (52, 53), they have not been precisely interpreted in the context of the naive/memory paradigm. Although CD45RA expression (and/or lack of expression of its largely reciprocal RO isoform) did indeed comprise the first reported criteria for naive T cell delineation in the human (15, 17), this phenotype has been subsequently shown to include a subset of Ag-experienced T cells in this species, especially among $CD8^+$ T cells (Refs. 22, 35, and 54–56 and see below), clearly invalidating the usefulness of this marker as a single criterion of naive/memory status in the human system. High expression of CD45RA on Ag-experienced cells is even more common in RM (up to 60% of memory cells with bright expression), including both $CD8^+$ and $CD4^+$ T cells, and in addition the $CD45RA^{low}$ memory subset overlaps the naive subset with respect to CD45RA intensity (see Fig. 1). The tandem use of CD62L reactivity with CD45RA also fails to reliably distinguish the naive subset: we have observed significant contamination (>30% in older animals) of the $CD45RA^+CD62L^+$ population with $CD95^{high}$ memory cells (data not shown). It is also important to note that surface CD62L is highly sensitive to proteolytic cleavage (29), often resulting in loss of expression on true naive cells (especially on stored or cryopreserved specimens) and thus, their misclassification. In contrast, the criteria developed here provide reliable separation of naive cells in both blood and secondary lymphoid tissues and are equally applicable to fresh, stored, and cryopreserved specimens.

The memory population, essentially all cells outside the naive cluster, included all IFN-γ production, RM CMV-specific responses, lung and intestinal lamina propria T cells (representative effector sites), and demonstrated relatively high in vivo proliferative activity (overall, ~10 times the naive subset). This population was quite low at birth, but in keeping with the expected result of postnatal Ag exposure, rapidly increased in the first few months of life. Cross-sectional analysis indicated that attainment of peripheral blood memory frequencies of 40–50%, the average frequency in adult human blood (32, 33), occurs within the first 2–3 years of life in RM. Thereafter, the rise in memory frequencies slows, but still, by middle adulthood (10–20 years), memory frequencies average ~70% for $CD4^+$ T cells and 80–90% for $CD8^+$ T cells.

Table III. *Summary: Phenotypic and functional characteristics of peripheral T cell subsets in RM*

	$CD4^+$ T Cells			$CD8^+$ T Cells		
	Naive	Central memory	Effector memory	Naive	Central memory	Effector memory
Phenotype						
CD95	−	+	+	−	+	+
CD28	+	Bright +	−	+	Bright +	−
β_7 integrin	+	Variable	−/dim +	+	Variable	Variable
CD11a	Dim +	Dim +	+	Dim +	+	Variable
CD62L	+	Variable	−	+	Variable	Majority –
CD45RA	+	Variable	Variable	+	Variable	Variable
Function						
IFN-γ production	−	+	+	−	+	+
CMV-specific response	−	Minority	Majority	−	Few	Vast majority
Localization						
Lymph node	+	Vast majority	Few	+	Vast majority	Few
Effector sites (lung, gut lamina propria)	−	Depleted	Enriched	−	Few	Vast majority
Development						
Frequency in neonatal blood	Vast majority	Few	−	Vast majority	Few	Very few
Turnover						
Ki-67 expression or BrdU uptake	Low	High	High	Low	High	High

These results suggest that RM, especially juvenile animals, may be exposed to more diverse pathogens more frequently than humans. Indeed, the frequencies of phenotypic memory cells (particularly of the $CD8^+$ subset) in neonatal (Fig. 3) and even late gestation fetal blood (data not shown), though low compared with later postnatal life, were much higher than we have observed in human umbilical cord blood (Refs. 19, 32, and 33, and L. J. Picker, personal observation), suggesting that these animals may experience more prenatal Ag exposure than humans as well. Accelerated natural Ag exposure and the resultant time-contracted nature of memory differentiation in RM is useful from the perspective of a model to study memory differentiation—the tempo of memory development is rapid enough for prospective experimental study. On the other hand, this rapid memory development (with its implication for high levels of ongoing immune activity) raises important caveats to interpretation of data generated in the extensive ongoing use of RM in SIV pathogenesis and vaccine studies. Many of the animals used for these studies are in the age range of rapid memory development, bringing up the question of whether the relative levels of immunologic activity and ongoing memory development in these animals differentially affects their response to vaccines and/or the course of SIV infection.

The RM memory population was characterized, as expected, by phenotypic diversity, but there were discernible patterns in this diversity, patterns with important functional correlates. Both $CD4^+$ and $CD8^+$ T memory cells demonstrated a subset primarily characterized by loss of CD28 expression with stereotyped phenotypic and functional features. $CD4^+CD28^-$ T cells were generally $CD11a^{high}$, $CD49d(\alpha_4\ integrin)^{high}$, $CD62L^-$, and β_7 $integrin^{-\ to\ low}$. $CD8^+CD28^-$ T cells were generally similar, except that this population also included a discrete β_7 $integrin^{bright}$, $CD11a^{low}$ subset. These phenotypic features suggest a population with enhanced ability to home to extralymphoid (effector) sites, either generally or, in the case of the β_7 $integrin^{bright}CD11a^{low}$ subset, specifically directed to intestinal lamina propria and related sites (5, 7). In keeping with this, the $CD28^-$ subset was directly shown to be significantly enriched in representative RM effector sites, lung and intestinal lamina propria (Fig. 8), in a homing receptor appropriate manner (e.g., β_7 $integrin^{bright}$ cells predominately in gut lamina propria; Fig. 2). We also demonstrated that $CD28^{-/dim}$ T cells accounted for the majority of T cells specific for epitopes encoded by the chronic pathogen RM CMV (Fig. 5 and Table II), and that this population appears with a delay in early memory development and progressively accumulates within the memory subset thereafter (Figs. 3 and 7).

These features are characteristic of the effector memory subset described in humans and rodents (8, 18, 22, 23, 30, 35–44), which has been envisioned as a terminally differentiated memory subset "trained" for direct anti-pathogen effector activity in extralymphoid sites. In humans, effector memory cells have been characterized by the largely overlapping $CD28^-$ and $CD27^-$ phenotypes and by "reversed" CD45 isoform expression (e.g., $CD45RA^{high}RO^{low}$). In RM, the CD27 and CD45RA criteria do not appear to apply. RM CD27 can be visualized by cross-reacting human CD27-specific Abs, but a definitive $CD27^-$ memory subset is not observed, and the variability of expression intensity that is observed does not correlate with CD28 expression or any of the other phenotypic correlates of the effector memory subset (data not shown). With regard to CD45RA, correlation with the $CD28^-$ subset is only observed for peripheral blood $CD4^+$ T memory cells, not $CD8^+$ memory cells or $CD4^+$ cells in effector sites. Moreover, the $CD8^+CD45RA^{++}$ subset does not accumulate with age. Taken together, these data are consistent with 1) the correlation of CD28 loss with a linear differentiation pathway among memory cells, and 2) the independent regulation of CD45RA (the expression of which may switch both on and off memory T cells in response to unknown signals).

The current paradigm for the homeostasis of the $CD28^-$ effector memory subset is that this subset, as a terminally differentiated population, manifests limited replicative capacity and derives from and is maintained by the differentiation of the secondary lymphoid tissue-based, replication competent, $CD28^+$ central memory subset (18, 22, 36–38, 57, 58). The stability of the $CD28^-$ subset has been somewhat controversial, with some studies suggesting it is relatively resistant to apoptosis, and others suggesting it is relatively sensitive (37, 40, 57). These hypotheses have largely been based on in vitro experimentation, and the in vivo physiology of this subset must be considered unknown. In this study, we provide some insight into this issue by the analysis of Ki-67 expression and BrdU uptake among RM T cells in general and these memory subsets in specific.

First, as indicated above, memory cells constitute the vast majority of cycling cells, with rates of Ki-67 expression or BrdU uptake ~10 times higher than the naive subset. This finding is in general agreement with several previous studies in RM (48, 50, 52), but the naive/memory delineation in these prior studies was

based on CD45RA alone or CD45RA/CD62L and thus may not have reliably separated these subsets (as discussed above). Second, simultaneous analysis of Ki-67 and BrdU incorporation after varying BrdU pulse periods suggested complete labeling of Ki-67$^+$ cells with 3- to 4-day pulses, and then loss of Ki-67 reactivity on the vast majority of labeled cells within ~1 wk after the pulse. These observations indicate that the vast majority of Ki-67$^+$ T cells in peripheral blood have undergone S phase in the preceding 3–4 days and few, if any, of these Ki-67$^+$ cells appear to have undergone cell cycle arrest. Moreover, they suggest that the proliferative activity of the majority of T cells is episodic, with cells entering cell cycle, undergoing a limited number of divisions, and then returning to G_o phase (i.e., most proliferating cells are not continuously cycling). Third, frequencies of labeled cells decline slowly over the washout period with little discernible change in BrdU staining, indicating that a substantial fraction of postdivision, recirculating T cells revert to the nonproliferative state and survive for many weeks. Re-entry of labeled cells into the cell cycle appeared to be stochastic, occurring at a frequency similar to that of unlabeled cells. Fourth, Ki-67 reactivity and BrdU incorporation following 1-, 3-, or 6-day BrdU pulses were not significantly different between the CD28$^-$ effector memory and the CD28$^+$ central memory subsets. Significant Ki-67 reactivity within the CD28$^-$ T cell subset has also been reported by Kaur et al. (52). In vitro maturation of CD28$^-$ T cells from CD28$^+$ precursors in humans takes many days to weeks (57, 58), and the delayed development of the CD28$^-$ T cell subset relative to overall memory population in RM suggests this differentiation process is not immediate in vivo either. Thus, the Ki-67 reactivity and BrdU uptake (after as little as 24 h of pulsing) exhibited by the CD28$^-$ effector memory subset is likely due to proliferation within this subset and not proliferation of CD28$^+$ central memory T cells with subsequent differentiation to a CD28$^-$ phenotype. Finally, decay rates of BrdU-labeled cells and BrdU staining intensities were similar among the CD28$^-$ and CD28$^+$ subsets, suggesting that either survival of these subsets was equivalent or that loss of CD28$^-$ memory cells is precisely compensated by differentiating (but nonproliferating) CD28$^+$ cells. Against this later interpretation was the observation that the decay of a steady-state IE-1-specific CD8$^+$ memory subset, which is predominantly CD28$^-$ and therefore lacks a significant CD28$^+$ central memory reservoir, was similar to the overall CD28$^-$ effector memory subset.

Overall, these observations strongly suggest that in vivo the CD28$^-$ effector memory subset is as replication capable and as intrinsically stable as the CD28$^+$ central memory subset, and therefore most likely constitutes a population capable of independent homeostasis. These data do not contradict the role of the CD28$^+$ central memory subset as a precursor of the effector memory subset, but do suggest that after this differentiation, maintenance of the effector memory population is not completely dependent on this differentiation. Given the vastly different tissue-homing preferences of central and effector memory subsets and the consequent differences in their microenvironmental "niches" (59), it is highly likely the homeostasis of these subsets is controlled by distinct regulatory influences. Thus, sequential linear differentiation of memory T cells—central memory to effector memory—may be accompanied not only by changes in function, but also by the development of independent mechanisms of population homeostasis, analogous to the independent homeostasis of naive vs total memory populations (59).

In summary, this report has defined and validated a new analytic paradigm for the definition of naive and memory T cells in RM and has delineated optimized approaches for the study of the function and homeostasis of these cells. Preliminary data indicate that all of the technical and analytic approaches defined here for RM work equivalently in cynomologous monkeys (*Macaca fascicularis*) as well (data not shown). These nonhuman primates provide a manipulable, time-contracted model of memory development that much more closely resembles the human system than rodent models. Moreover, the application of these analytic tools to nonhuman primate infectious disease and vaccine models will facilitate determination of protective thresholds for T cell immunity and their maintenance over time.

References

1. Notermans, D. W., N. G. Pakker, D. Hamann, N. A. Foudraine, R. H. Kauffmann, P. L. Meenhorst, J. Goudsmit, M. T. Roos, P. T. Schellekens, F. Miedema, and S. A. Danner. 1999. Immune reconstitution after 2 years of successful potent antiretroviral therapy in previously untreated human immunodeficiency virus type 1- infected adults. *J. Infect. Dis. 180:1050.*
2. Collins, R. H., Jr., M. Sackler, C. J. Pitcher, S. L. Waldrop, G. B. Klintmalm, R. Jenkins, and L. J. Picker. 1997. Immune reconstitution with donor-derived memory/effector T cells after orthotopic liver transplantation. *Exp. Hematol. 25: 147.*
3. Rabin, R. L., M. Roederer, Y. Maldonado, A. Petru, and L. A. Herzenberg. 1995. Altered representation of naive and memory CD8 T cell subsets in HIV-infected children. *J. Clin. Invest. 95:2054.*
4. De Rosa, S. C., L. A. Herzenberg, and M. Roederer. 2001. 11-color, 13-parameter flow cytometry: identification of human naive T cells by phenotype, function, and T-cell receptor diversity. *Nat. Med. 7:245.*
5. Picker, L. J., and M. H. Siegelman. 1999. Lymphoid organs and tissues. In *Fundamental Immunology*, 4th Ed., Chapter 14. W. E. Paul, ed. Lippincott-Raven, Philadelphia, p. 479.
6. Pakker, N. G., E. D. Kroon, M. T. Roos, S. A. Otto, D. Hall, F. W. Wit, D. Hamann, M. E. van der Ende, F. A. Claessen, R. H. Kauffmann, et al. 1999. Immune restoration does not invariably occur following long-term HIV-1 suppression during antiretroviral therapy: INCAS Study Group. *AIDS 13:203.*
7. Butcher, E. C., and L. J. Picker. 1996. Lymphocyte homing and homeostasis. *Science 272:60.*
8. Lanzavecchia, A., and F. Sallusto. 2000. Dynamics of T lymphocyte responses: intermediates, effectors, and memory cells. *Science 290:92.*
9. Tough, D. F., and J. Sprent. 1994. Turnover of naive- and memory-phenotype T cells. *J. Exp. Med. 179:1127.*
10. Michie, C. A., A. McLean, C. Alcock, and P. C. L. Beverley. 1992. Lifespan of human lymphocyte subsets defined by CD45 isoforms. *Nature 360:264.*
11. Tanchot, C., A. Le Campion, S. Leaument, N. Dautigny, and B. Lucas. 2001. Naive CD4+ lymphocytes convert to anergic or memory-like cells in T cell-deprived recipients. *Eur. J. Immunol. 31:2256.*
12. Picker, L. J., J. R. Treer, B. Ferguson-Darnell, P. A. Collins, P. R. Bergstresser, and L. W. Terstappen. 1993. Control of lymphocyte recirculation in man. II. Differential regulation of the cutaneous lymphocyte-associated antigen, a tissue-selective homing receptor for skin-homing T cells. *J. Immunol. 150:1122.*
13. Picker, L. J., J. R. Treer, B. Ferguson-Darnell, P. A. Collins, D. Buck, and L. W. Terstappen. 1993. Control of lymphocyte recirculation in man. I. Differential regulation of the peripheral lymph node homing receptor L-selection on T cells during the virgin to memory cell transition. *J. Immunol. 150:1105.*
14. Teraki, Y., and L. J. Picker. 1997. Independent regulation of cutaneous lymphocyte-associated antigen expression and cytokine synthesis phenotype during human CD4$^+$ memory T cell differentiation. *J. Immunol. 159:6018.*
15. Sanders, M. E., M. W. Makagoba, S. O. Sharrow, D. Stephany, T. A. Springer, H. A. Young, and S. Shaw. 1988. Human memory T lymphocytes express increased levels of three cell adhesion molecules (LFA-3, CD2, and LFA-1) and three other molecules (UCHL1, CDw29, and Pgp-1) and have enhanced IFN-γ production. *J. Immunol. 140:1401.*
16. Bleul, C. C., L. Wu, J. A. Hoxie, T. A. Springer, and C. R. Mackay. 1997. The HIV coreceptors CXCR4 and CCR5 are differentially expressed and regulated on human T lymphocytes. *Proc. Natl. Acad. Sci. USA 94:1925.*
17. Akbar, A. N., L. Terry, A. Timms, P. C. L. Beverely, and G. Janossy. 1988. Loss of CD45R and gain of UCHL1 reactivity is a feature of primed T cells. *J. Immunol. 140:2171.*
18. Sallusto, F., D. Lenig, R. Forster, M. Lipp, and A. Lanzavecchia. 1999. Two subsets of memory T lymphocytes with distinct homing potentials and effector functions. *Nature 401:708.*
19. Picker, L. J., L. W. Terstappen, L. S. Rott, P. R. Streeter, H. Stein, and E. C. Butcher. 1990. Differential expression of homing-associated adhesion molecules by T cell subsets in man. *J. Immunol. 145:3247.*
20. McCune, J. M., M. B. Hanley, D. Cesar, R. Halvorsen, R. Hoh, D. Schmidt, E. Wieder, S. Deeks, S. Siler, R. Neese, and M. Hellerstein. 2000. Factors influencing T-cell turnover in HIV-1-seropositive patients. *J. Clin. Invest. 105:R1.*
21. Pakker, N. G., D. W. Notermans, R. J. de Boer, M. T. Roos, F. de Wolf, A. Hill, J. M. Leonard, S. A. Danner, F. Miedema, and P. T. Schellekens. 1998. Biphasic kinetics of peripheral blood T cells after triple combination therapy in HIV-1 infection: a composite of redistribution and proliferation. *Nat. Med. 4:208.*
22. Hamann, D., P. A. Baars, M. H. Rep, B. Hooibrink, S. R. Kerkhof-Garde, M. R. Klein, and R. A. van Lier. 1997. Phenotypic and functional separation of memory and effector human CD8$^+$ T cells. *J. Exp. Med. 186:1407.*

23. Masopust, D., V. Vezys, A. L. Marzo, and L. Lefrancois. 2001. Preferential localization of effector memory cells in nonlymphoid tissue. *Science 291:2413.*
24. Veazey, R. S., M. Rosenzweig, D. E. Shvetz, D. R. Pauley, M. DeMaria, L. V. Chalifoux, R. P. Johnson, and A. A. Lackner. 1997. Characterization of gut-associated lymphoid tissue (GALT) of normal rhesus macaques. *Clin. Immunol. Immunopathol. 82:230.*
25. Maecker, H. T., H. S. Dunn, M. A. Suni, E. Khatamzas, C. J. Pitcher, T. Bunde, N. Persaud, W. Trigona, T.-M. Fu, E. Sinclair, et al. 2001. Use of overlapping peptide mixtures as antigens for cytokine flow cytometry. *J. Immunol. Methods 255:27.*
26. Waldrop, S. L., K. A. Davis, V. C. Maino, and L. J. Picker. 1998. Normal human $CD4^+$ memory T cells display broad heterogeneity in their activation threshold for cytokine synthesis. *J. Immunol. 161:5284.*
27. Waldrop, S. L., C. J. Pitcher, D. M. Peterson, V. C. Maino, and L. J. Picker. 1997. Determination of antigen-specific memory/effector $CD4^+$ T cell frequencies by flow cytometry: evidence for a novel, antigen-specific homeostatic mechanism in HIV-associated immunodeficiency. *J. Clin. Invest. 99:1739.*
28. Terstappen, L. W., S. Huang, and L. J. Picker. 1992. Flow cytometric assessment of human T-cell differentiation in thymus and bone marrow. *Blood 79:666.*
29. Kishimoto, T. K., M. A. Jutila, and E. C. Butcher. 1990. Identification of a human peripheral lymph node homing receptor: a rapidly down-regulated adhesion molecule. *Proc. Natl. Acad. Sci. USA 87:2244.*
30. Reinhardt, R. L., A. Khoruts, R. Merica, T. Zell, and M. K. Jenkins. 2001. Visualizing the generation of memory CD4 T cells in the whole body. *Nature 410:101.*
31. Picker, L. J., R. J. Martin, A. Trumble, L. S. Newman, P. A. Collins, P. R. Bergstresser, and D. Y. Leung. 1994. Differential expression of lymphocyte homing receptors by human memory/effector T cells in pulmonary versus cutaneous immune effector sites. *Eur. J. Immunol. 24:1269.*
32. Douek, D. C., R. D. McFarland, P. H. Keiser, E. A. Gage, J. M. Massey, B. F. Haynes, M. A. Polis, A. T. Haase, M. B. Feinberg, J. L. Sullivan, et al. 1998. Changes in thymic function with age and during the treatment of HIV infection. *Nature 396:690.*
33. McFarland, R. D., D. C. Douek, R. A. Koup, and L. J. Picker. 2000. Identification of a human recent thymic emigrant phenotype. *Proc. Natl. Acad. Sci. USA 97: 4215.*
34. Picker, L. J., M. K. Singh, Z. Zdraveski, J. R. Treer, S. L. Waldrop, P. R. Bergstresser, and V. C. Maino. 1995. Direct demonstration of cytokine synthesis heterogeneity among human memory/effector T cells by flow cytometry. *Blood 86:1408.*
35. Kern, F., E. Khatamzas, I. Surel, C. Frommel, P. Reinke, S. L. Waldrop, L. J. Picker, and H. D. Volk. 1999. Distribution of human CMV-specific memory T cells among the $CD8^{pos.}$ subsets defined by CD57, CD27, and CD45 isoforms. *Eur. J. Immunol. 29:2908.*
36. Champagne, P., G. S. Ogg, A. S. King, C. Knabenhans, K. Ellefsen, M. Nobile, V. Appay, G. P. Rizzardi, S. Fleury, M. Lipp, et al. 2001. Skewed maturation of memory HIV-specific CD8 T lymphocytes. *Nature 410:106.*
37. Posnett, D. N., J. W. Edinger, J. S. Manavalan, C. Irwin, and G. Marodon. 1999. Differentiation of human CD8 T cells: implications for in vivo persistence of $CD8^+$ $CD28^-$ cytotoxic effector clones. *Int. Immunol. 11:229.*
38. Nociari, M. M., W. Telford, and C. Russo. 1999. Postthymic development of $CD28^-CD8^+$ T cell subset: age-associated expansion and shift from memory to naive phenotype. *J. Immunol. 162:3327.*
39. Weekes, M. P., A. J. Carmichael, M. R. Wills, K. Mynard, and J. G. Sissons. 1999. Human $CD28^-CD8^+$ T cells contain greatly expanded functional virus-specific memory CTL clones. *J. Immunol. 162:7569.*
40. Vallejo, A. N., M. Schirmer, C. M. Weyand, and J. J. Goronzy. 2000. Clonality and longevity of $CD4^+CD28^{null}$ T cells are associated with defects in apoptotic pathways. *J. Immunol. 165:6301.*
41. Hol, B. E., R. Q. Hintzen, R. A. Van Lier, C. Alberts, T. A. Out, and H. M. Jansen. 1993. Soluble and cellular markers of T cell activation in patients with pulmonary sarcoidosis. *Am. Rev. Respir. Dis. 148:643.*
42. Hintzen, R. Q., R. de Jong, S. M. Lens, M. Brouwer, P. Baars, and R. A. van Lier. 1993. Regulation of CD27 expression on subsets of mature T-lymphocytes. *J. Immunol. 151:2426.*
43. De Rie, M. A., I. Cairo, R. A. Van Lier, and J. D. Bos. 1996. Expression of the T-cell activation antigens CD27 and CD28 in normal and psoriatic skin. *Clin. Exp. Dermatol. 21:104.*
44. Roos, M. T., R. A. van Lier, D. Hamann, G. J. Knol, I. Verhoofstad, D. van Baarle, F. Miedema, and P. T. Schellekens. 2000. Changes in the composition of circulating $CD8^+$ T cell subsets during acute Epstein-Barr and human immunodeficiency virus infections in humans. *J. Infect. Dis. 182:451.*
45. Lempicki, R. A., J. A. Kovacs, M. W. Baseler, J. W. Adelsberger, R. L. Dewar, V. Natarajan, M. C. Bosche, J. A. Metcalf, R. A. Stevens, L. A. Lambert, et al. 2000. Impact of HIV-1 infection and highly active antiretroviral therapy on the kinetics of $CD4^+$ and $CD8^+$ T cell turnover in HIV-infected patients. *Proc. Natl. Acad. Sci. USA 97:13778.*
46. Reome, J. B., D. S. Johnston, B. K. Helmich, T. M. Morgan, N. Dutton-Swain, and R. W. Dutton. 2000. The effects of prolonged administration of 5-bromodeoxyuridine on cells of the immune system. *J. Immunol. 165:4226.*
47. Gerdes, J., H. Lemke, H. Baisch, H. H. Wacker, U. Schwab, and H. Stein. 1984. Cell cycle analysis of a cell proliferation-associated human nuclear antigen defined by the monoclonal antibody Ki-67. *J. Immunol. 133:1710.*
48. Mohri, H., S. Bonhoeffer, S. Monard, A. S. Perelson, and D. D. Ho. 1998. Rapid turnover of T lymphocytes in SIV-infected rhesus macaques. *Science 279:1223.*
49. DeMaria, M. A., M. Casto, M. O'Connell, R. P. Johnson, and M. Rosenzweig. 2000. Characterization of lymphocyte subsets in rhesus macaques during the first year of life. *Eur. J. Haematol. 65:245.*
50. Rosenzweig, M., M. A. DeMaria, D. M. Harper, S. Friedrich, R. K. Jain, and R. P. Johnson. 1998. Increased rates of $CD4^+$ and $CD8^+$ T lymphocyte turnover in simian immunodeficiency virus-infected macaques. *Proc. Natl. Acad. Sci. USA 95:6388.*
51. Veazey, R. S., K. G. Mansfield, I. C. Tham, A. C. Carville, D. E. Shvetz, A. E. Forand, and A. A. Lackner. 2000. Dynamics of CCR5 expression by $CD4^+$ T cells in lymphoid tissues during simian immunodeficiency virus infection. *J. Virol. 74:11001.*
52. Kaur, A., C. L. Hale, S. Ramanujan, R. K. Jain, and R. P. Johnson. 2000. Differential dynamics of $CD4^+$ and $CD8^+$ T-lymphocyte proliferation and activation in acute simian immunodeficiency virus infection. *J. Virol. 74:8413.*
53. Kuroda, M. J., J. E. Schmitz, W. A. Charini, C. E. Nickerson, C. I. Lord, M. A. Forman, and N. L. Letvin. 1999. Comparative analysis of cytotoxic T lymphocytes in lymph nodes and peripheral blood of simian immunodeficiency virus-infected rhesus monkeys. *J. Virol. 73:1573.*
54. Arlettaz, L., C. Barbey, F. Dumont-Girard, C. Helg, B. Chapuis, E. Roux, and E. Roosnek. 1999. CD45 isoform phenotypes of human T cells: $CD4^+CD45RA^-RO^+$ memory T cells re-acquire CD45RA without losing CD45RO. *Eur. J. Immunol. 29:3987.*
55. Faint, J. M., N. E. Annels, S. J. Curnow, P. Shields, D. Pilling, A. D. Hislop, L. Wu, A. N. Akbar, C. D. Buckley, P. A. Moss, et al. 2001. Memory T cells constitute a subset of the human $CD8^+CD45RA^+$ pool with distinct phenotypic and migratory characteristics. *J. Immunol. 167:212.*
56. Wills, M. R., A. J. Carmichael, M. P. Weekes, K. Mynard, G. Okecha, R. Hicks, and J. G. Sissons. 1999. Human virus-specific $CD8^+$ CTL clones revert from $CD45RO^{high}$ to $CD45RA^{high}$ in vivo: $CD45RA^{high}CD8^+$ T cells comprise both naive and memory cells. *J. Immunol. 162:7080.*
57. Borthwick, N. J., M. Lowdell, M. Salmon, and A. N. Akbar. 2000. Loss of CD28 expression on $CD8^+$ T cells is induced by IL-2 receptor γ chain signalling cytokines and type I IFN, and increases susceptibility to activation-induced apoptosis. *Int. Immunol. 12:1005.*
58. Labalette, M., E. Leteurtre, C. Thumerelle, C. Grutzmacher, B. Tourvieille, and J. P. Dessaint. 1999. Peripheral human $CD8^+CD28^+$ T lymphocytes give rise to $CD28^-$ progeny, but IL-4 prevents loss of CD28 expression. *Int. Immunol. 11: 1327.*
59. Freitas, A. A., and B. Rocha. 2000. Population biology of lymphocytes: the flight for survival. *Annu. Rev. Immunol. 18:83.*